Office of Naval Research

DEPARTMENT OF THE NAVY

Contract N6onr_24420 (NR 062_059)

A FREE STREAMLINE THEORY FOR TWO-DIMENSIONAL FULLY CAVITATED HYDROFOILS

T. Yao-tsu Wu

Hydrodynamics Laboratory

CALIFORNIA INSTITUTE OF TECHNOLOGY

Pasadena, California

Report No. 21-17

July, 1955

A FREE STREAMLINE THEORY FOR TWO-DIMENSIONAL FULLY CAVITATED HYDROFOILS

I. INTRODUCTION

The problem of cavity flows received attention early in the development of hydrodynamics because of its occurrence in high speed motion of solid bodies in water. Many previous works in this field were mainly concerned with the calculation of drag in a cavitating flow. The lifting problem with a cavity (or wake) arose later in the applications of water pumps, marine propellers, stalling airfoils, and hydrofoil crafts. Although several formulations of the problem of lift in cavity flows have been pointed out before,[1-3] these theories have not yet been developed to yield general results in explicit form so that a unified discussion can be made.

The problems of cavitating flow with finite cavity demand an extension of the classical Helmholtz free boundary theory for which the cavity is infinite in extent. For this purpose, several self-consistent models have been introduced, all aiming to account for the cavity base pressure which is in general always less than the free stream pressure. In the Helmholtz-Kirchhoff flow these two pressures are assumed equal.

Of all these existing models, three significant ones may be mentioned here. The first representation of a finite cavity was proposed by Riabouchinsky[4]

in which the finite cavity is obtained by introducing an "image" obstacle downstream of the real body. A different representation in which a reentrant jet is postulated was suggested by Prandtl, Wagner, and was later considered by Kreisel[5] and was further extended by Gilbarg and Serrin.[3] Another representation of a free streamline flow with the base pressure different from the free stream pressure was proposed recently by Roshko.[6] In this model the base pressure in the wake (or cavity) near the body can take any assigned value. From a certain point in the wake, which can be determined from the theory, the flow downstream is supposed to be dissipated in such a way that the pressure increases gradually from the assigned value to that of the free stream in a strip parallel to the free stream. Apparently this model was also considered independently by Eppler[7] in some generality. Other alternatives to these models have also been proposed,[8] but they do not differ so basically from the above three models that they need to be mentioned here specifically. The mathematical solutions to the problem of flow past a flat plate set normal to the stream have been carried out for these three models.[9,6] All the theories are found to give essentially the same results over the practical range of the wake underpressure. That such agreement is to be expected can be indicated, without the detailed solutions for the various models, from consideration of their underlying physical significance, as will be discussed in the next section.

In the present work the free streamline theory is extended and applied to the lifting problem for two-dimensional hydrofoils with a fully cavitating wake. The analysis is carried out by using the Roshko model to approximate the wake far downstream. The reason for using this model is mainly because of its mathematical simplicity as compared with the Riabouchinsky model, or the reentrant jet model. In fact, it can be verified that these different models

all yield practically the same result, as in the pure drag case; the deviation from the results of one model to another is not appreciable up to second order small quantities. The mathematical considerations here, as in the classical theory, depend on the conformal mapping of the complex velocity plane into the plane of complex potential. By using a generalization of Levi-Civita's method for curved barriers in cavity flows, the flow problem for curved hydrofoils is finally reduced to a nonlinear boundary value problem for an analytic function defined in the upper half of a unit circle to which the Schwarz's principle of reflection can be applied. The problem is then solved by using the expansion of this analytic function inside the unit circle together with the boundary conditions in the physical plane. In order to avoid the difficulty in determining the separation point of the free streamline from a hydrofoil with blunt nose, the hydrofoils investigated here are those with sharp leading and trailing edges which are assumed to be the separation points. Except for this limitation, the present nonlinear theory is applicable to hydrofoils of any geometric profile, operating at any cavitation number, and for almost all angles of attack as long as the wake has a fully cavitating configuration.

As two typical examples, the problem is solved in explicit form for the circular arc and the flat plate for which the various flow quantities are expressed by simple formulas. From the final result the various effects, such as that of cavitation number, camber of the profile and the attack angle, are discussed in detail. It is also shown that the present theory is in good agreement with the experiment.

II. REMARKS ON MODELS IN FREE STREAMLINE THEORY

The total force (drag and lift for two-dimensional flows) exerted by the fluid on a solid body may of course be expressed as an integral of the local

force, which consists of both the pressure and viscous stresses over the surface of the solid. However, it is also possible to express the total force in terms of integrals over surfaces at a distance from the body by applying the momentum theory. In the case of the real fluid flow past a bluff body, experimental observations indicate that the discontinuous surfaces in the flow, or free streamlines, are actually thin shear layers, into which the vorticity is fed from the boundary layer in front of the separation point. The shear layers in general do not continue smoothly far downstream, but roll up to form vortices, alternately on each side with a certain frequency. These vortices diffuse rapidly and are eventually dissipated in the wake. With a constant upstream velocity, the wake flow is thus only stationary in the mean. Because of this complicated wake flow, it seems rather fruitless to apply the momentum theory which requires a detailed consideration of the free streamlines at infinity. A more realistic way to formulate the problem is thus to obtain a solution which is accurate near the body by taking appropriate consideration of the cavity pressure. It is physically plausible that the detailed structure of the wake far downstream has indeed negligible influence upon the flow field near the body. Consequently, one may represent the dissipative wake flow by an equivalent model of potential flow, if properly chosen.

The general character of cavity flows depends on the value of the cavitation number σ which is defined by

$$\sigma = (P - p_\sigma)/(\tfrac{1}{2}\rho U^2) \tag{2.1}$$

where P denotes the pressure of the undisturbed free stream, U is its relative velocity, ρ is the fluid density, and p_σ is the pressure of the vapor or gas in the cavity. Physical cavities usually have finite length and positive

cavitation number ($\sigma > 0$, or $p_\sigma < P$). Some mathematical formulations have been suggested previously to investigate the possibility for obtaining the solution of steady cavity flows of ideal fluid satisfying the following conditions:

(i) the cavitation number is greater than zero, $\sigma > 0$, or $p_\sigma < P$;

(ii) the cavity pressure is uniform throughout the cavity;

(iii) the pressure of the fluid is nowhere less than the cavity pressure;

(iv) the pressure is continous across the cavity boundary.

The first two conditions are imposed because of their physical reality ($\sigma = 0$ case is physically unreal). The third condition follows from the potential flow theory that the velocity cannot have a maximum in the interior of the flow field. The last condition states that the interface between two phases of fluid cannot withstand any pressure jump. It then follows from (ii) that the free streamlines are surfaces of constant velocity; also, (iii) always implies that the cavity boundary is convex towards the interior flow. Application of Bernoulli's equation with condition (iii) shows that the velocity is maximum on the cavity boundary. It should be noted that these conditions differ only in (i) from the classical theory, for which $\sigma = 0$ (or $p_\sigma = P$), corresponding to an infinitely long cavity. If the flow is restricted to be everywhere potential flow, then the cavity cannot have finite length for $\sigma \geqslant 0$. For if the cavity were to close up at the rear end by itself, then the free streamlines from two sides of the body should meet either at a stagnation point from opposite directions or with a cusp in the downstream direction. The first conjecture contradicts (ii), while the second alternative violates (iii). Though the streamlines may reverse in direction and form a reentrant jet, as often observed, the jet cannot terminate in the physical plane. The above argument indicates the need of models of potential flow to represent the dissipative

wake downstream if the formulation of the problem is to be retained within the scope of potential theory.

Now the problem of flow past a two-dimensional flat plate set normal to the stream, forming a finite cavity, shall be reviewed to exhibit the characteristics of these models. In the model of Riabouchinsky, an image plate A' (see Fig. 1a) is put downstream of the real plate A. The free streamlines run from A to A' and the flow field is assumed irrotational everywhere. The total force on the pair of plates then vanishes, but the calculation of the drag on A alone yields the following approximate expression for the drag coefficient:

$$C_D(\sigma) \cong \left\{ 1 + \sigma + [8(\pi+4)]^{-1}\sigma^2 \right\} C_D(0) \cong (1+\sigma)\, C_D(0) \tag{2.2}$$

where $C_D(0) = 2\pi/(4 + \pi) = 0.88$ is the classical Helmholtz solution for $\sigma = 0$. The physical significance of the image plate can perhaps be justified by the following argument. In a coordinate system where the fluid at infinity is at rest, the force holding A' does an amount of negative work, equal to $W = - DU$, where D is the drag on A and U is the speed of the traveling plates. The coefficient of work defined by $C_w = W/(\frac{1}{2}\rho U^3 \ell)$, where ℓ is the plate width, then equals $-C_D$. Now if the wake is approximated by a vortex street and C_D be calculated from the vortex energy shed into the wake, the result is (see Ref. 10, p. 557)

$$C_D = \frac{a}{\ell}\left[1.59\, \frac{U_s}{U} - 0.63 \left(\frac{U_s}{U}\right)^2 \right], \tag{2.3}$$

where a is the spacing between consecutive vortices in the same row and U_S is the receding velocity of the vortices relative to the undisturbed flow. If the air is taken to be the fluid medium (because of more data available in

this case), the measured underpressure[11] corresponds to $\sigma = 1.2$ for which Eq. (2.2) gives $C_D = 1.93$. For the same flow, Heisenberg[10] showed, by using some representative experimental values, that Eq. (2.3) yields $C_D = 1.82$. Thus, the work done by the image plate, even though it does not exist in reality, provides a good representation of the energy shed to the wake, which should be removed from the flow if the flow is assumed to be potential. It should be noted that the result Eq. (2.2) together with the assumed flow configuration actually imposes on A' a certain restriction that A' must be of the same size as A. Now when asymmetric bodies, such as the lifting plate, are considered, a question arises whether the image body should be in symmetry with respect to a plane normal to the stream or only to a point in the cavity. In the former case, the physical reasoning suggests that a circulation around the cavity is necessary to generate a total lift on the pair of bodies; while in the later case, the potential is continuous everywhere in the fluid. A clarification of this vague point certainly seems necessary.

In the reentrant jet model, the free streamlines reverse direction at the rear of the cavity to form a jet which flows upstream in the cavity (see Fig. 1b) and is supposed not to impinge on the real body but is removed mathematically by allowing it to flow on a second Riemann sheet in the physical plane to infinity. Thus, in the original physical plane, the point infinity acts like a doublet plus a source, while the jet represents a sink. Physically, the jet momentum carried away from the first sheet is then closely associated with the energy dissipated in the wake. For even though the jet can usually be observed, it is rather weakened by the turbulent mixing, at least its observed width is much smaller than its theoretical value. For the flat plate flow, the theory yields for $C_D(\sigma)$ the same formula as Eq. (2.2), the jet

width is $0.22(1+\sigma/4)$ of the plate width. In the lifting problems, it can be shown from consideration of momentum that the jet will turn in direction and eventually flow towards the downstream on the second sheet for small enough attack angles.

In Roshko's dissipation model, the flow past a bluff body is considered in two parts. Near the body it is described by the free streamline theory to allow a possible adjustment of the underpressure. The flow farther downstream is described by an equivalent potential flow so that its pressure increases continuously to the free stream value as it approaches infinity in a strip parallel to the free stream (see Fig. 1c). In this manner, the actual dissipative wake flow is represented; the detailed mechanism according to which the flow is dissipated is immaterial. Thus, it can be seen that this model is actually closer to the physical fact than the other models for the air flow past bluff bodies. However, this model applies equally well to cavity flows if the wake in front of the dissipation range is considered to be the front half of the cavity. By using this theory, the solution of $C_D(\sigma)$ on the flat plate differs from the previous two solutions, Eq. (2.2), only slightly by a term of $0(\sigma^2)$. Moreover, for the lifting problems, the assumption that the dissipative wake is parallel to the free stream is still physically sound and hence needs no further modification.

To summarize, all these models have one essential feature in common: they are aimed to give a satisfactory description of the flow near the body by making possible an adjustment of the base pressure and thereby removing a serious limitation in the classical theory. For this reason, it should not be expected that these solutions of the flow field shall describe the wake far downstream. The freedom of adjusting the base pressure, therefore, yields

a family of solutions containing one parameter which can be expressed in terms of σ. For pure drag problems, the agreement of these theories in that they all yield the result Eq. (2.2) can be explained also from consideration of the hodograph involved (see Fig. 1 and Refs. 12, 13). However, it should be pointed out that for lifting problems the linear relation in σ for C_L and C_D such as given by Eq. (2.2) becomes invalid for moderate and small attack angles as will be shown by the present analysis. Consequently, the problem of calculating $C_L(\sigma)$ and $C_D(\sigma)$ cannot be reduced to the calculation of $C_L(0)$ and $C_D(0)$ for a given geometric configuration, as is usually done in pure drag problems.

With respect to the mathematical details involved in the analysis, these models differ in simplicity to some extent, especially for the lifting case. In Riabouchinsky's theory, some numerical integration containing elliptical integrals are required. Although the results obtained by using the reentrant jet model are expressible in terms of elementary functions, the Roshko model is still simpler in many respects.

III. FORMULATION OF THE PROBLEM

The free streamline theory is applied here to investigate the steady, two-dimensional flow at a given attack angle α past a hydrofoil with a fully cavitating wake. The leading and trailing edges of the hydrofoil are assumed to be sharp and the flow configurations concerned are such that free streamlines separate from the hydrofoil at these sharp edges, but otherwise the wetted side of the hydrofoil may have any continuous profile. After the cavity is fully developed, the thickness of the hydrofoil has no effect on the flow and, therefore, the hydrofoil will be assumed to be of zero thickness. The Roshko model (see previous sections) will be used to approximate the wake far

downstream. The flow in the physical space (or z-plane, where $z = x + iy$ with x parallel to the free stream) is shown in Fig. 2. Outside the wake the flow is assumed to be everywhere irrotational. Thus, from the complex potential

$$W(z) = \varphi(x,y) + i\,\psi(x,y)\,,$$

the complex velocity w can be derived as

$$w(z) = dW/dz = u - iv = q\,e^{-i\theta},$$

where q, θ are the magnitude and direction of the velocity field. Here, the velocity at separation is normalized to $q = 1$, and remains at this value along the free streamlines until the latter reach points D and D' where $\theta = 0$. Downstream of these two points, the free streamlines keep parallel to the free stream on DE' and $D'E'$ along which q decreases from unity back to the free stream value U. In order that the cavitation number of the flow be σ (see Eq. (2.1) for its definition) with $q = 1$ on AD and BD', U takes the value $(1+\sigma)^{-1/2}$, as can be shown by applying Bernoulli's equation

$$p + \tfrac{1}{2}\rho q^2 = P + \tfrac{1}{2}\rho U^2.$$

The mathematical problem can be treated by finding the conformal transformation which maps the W-plane into the w-plane. From this relation the physical plane can be deduced by an integration

$$z = \int dW/w$$

We introduce to W a transformation in ζ which is given by

$$\sqrt{W} = -b\left[\cos\beta + \tfrac{1}{2}(\zeta + \zeta^{-1})\right] \qquad (3.1)$$

where

$$b = \tfrac{1}{2}(b_1 + b_2), \qquad \cos\beta = (b_2 - b_1)/(b_1 + b_2),$$

and b_1 and b_2 are two positive quantities defined by

$$W_A = b_1^2, \qquad W_B = b_2^2 e^{2\pi i}.$$

This transformation maps the entire flow in the W-plane into the interior of the upper semi-circle of unit radius in the ζ-plane. The barrier ACB corresponds to the semi-circle $|\zeta| = 1$, $0 \le \arg \zeta \le \pi$, and the free streamlines ADE' and $BD'E'$ map on to the two halves of the diameter along the real axis. The approaching streamline EC leaves $\zeta = 0$ perpendicular to the real axis and approaches C along the direction $\arg \zeta = \pi - \beta$.

Because of the way the nonlinear boundary conditions are specified in the z-plane (that is, with θ described on the barrier and q given on the free streamlines), we introduce the variable

$$\omega = i \log w = \theta + i \log q \equiv \theta + i\tau.$$

The flow in the ω-plane is sketched in Fig. 2. The jump in the real component θ of ω at C, where $\tau = -\infty$, follows from the fact that the two branches of the streamlines at the stagnation point C in the z-plane are orthogonal. The notch DED' in the ω-plane results from the assumption introduced in this model. At E, $\omega_E = -i\epsilon$ where $\epsilon = \frac{1}{2}\log(1+\sigma)$. This notch can be removed by the transformation

$$\Omega = -\sqrt{\omega^2 + \epsilon^2}, \qquad \epsilon = \tfrac{1}{2}\log(1+\sigma). \tag{3.2}$$

It should be noted that the present case ($\sigma > 0$) differs from the classical theory ($\sigma = 0$) only by the last transformation. When $\sigma = 0$, Ω and $-\omega$ become identical and the problem reduces to the classical Levi-Civita problem.

It follows from the jump condition of $\Omega(\zeta)$ at $\zeta_c = e^{i(\pi-\beta)}$ that the analytic function $\Omega(\zeta)$ has a logarithmic singularity at ζ_c and is regular elsewhere within the semi-circle. Moreover, we note that $\Omega(\zeta)$ is real for

real ζ, and therefore the function $\Omega(\zeta)$ can be continued analytically over the lower half of the unit circle by applying Schwarz's principle of symmetry. More precisely, since $\Omega(0) = 0$, we may express the function $\Omega(\zeta)$ by

$$\Omega(\zeta) = i \log\left[(1+\zeta e^{-i\beta})/(1+\zeta e^{i\beta})\right] + \sum_{n=1}^{\infty} A_n \zeta^n. \tag{3.3}$$

The first term on the right-hand side represents the singular part of $\Omega(\zeta)$ while the series denotes the expansion of an analytic function, regular and hence convergent, in and on the unit circle. The coefficients, A_n's, are real and can be determined in principle from the geometry of the barrier ACB (see Sec. 4). Near the origin, we have

$$\Omega(\zeta) = \sum_{n=1}^{\infty} \left[(-1)^{n+1} \frac{2}{n} \sin n\beta + A_n\right] \zeta^n \equiv \sum_{n=1}^{\infty} a_n \zeta^n, \qquad (|\zeta|<1). \tag{3.4}$$

On the barrier, where $\zeta = e^{i\eta}$, $0 \le \eta \le \pi$, we have

$$T(\eta) = \mathcal{I}m\,\Omega = \frac{1}{2} \log \frac{1+\cos(\eta-\beta)}{1+\cos(\eta+\beta)} + \sum_{n=1}^{\infty} A_n \sin n\eta\,; \tag{3.5a}$$

$$\Theta(\eta) = \mathcal{R}e\,\Omega = \beta_0 + \beta + \sum_{n=1}^{\infty} A_n \cos n\eta\,; \tag{3.5b}$$

where $\beta_0 = 0$ for $0 \le \eta < (\pi-\beta)$ and $\beta_0 = -\pi$ for $(\pi-\beta) < \eta \le \pi$. Now from the definition of ω and the expression of W in terms of ζ, (3.1), the physical plane $z(\zeta)$ can be obtained by integrating

$$dz = e^{i\omega} dW = \frac{b^2}{2} \exp\left\{-i(\Omega^2-\epsilon^2)^{1/2}\right\} \left(\zeta + \frac{1}{\zeta} + 2\cos\beta\right)\left(\zeta - \frac{1}{\zeta}\right) \frac{d\zeta}{\zeta} \tag{3.6}$$

which, in particular, reduces on the wetted wall, $\zeta = e^{i\eta}$, to

$$z = 2b^2 \int_{\eta}^{\pi-\beta} e^{-i(\Omega^2-\epsilon^2)^{1/2}} (\cos\eta + \cos\beta) \sin\eta\, d\eta. \tag{3.7}$$

The arc length of the barrier along CA or CB can be determined from

$$s = \int_{\eta}^{\pi-\beta} \frac{|dz|}{d\eta} d\eta = 2b^2 \int_{\eta}^{\pi-\beta} e^{-\tau(\eta)} (\cos\eta + \cos\beta) \sin\eta\, d\eta\,; \tag{3.8}$$

and the total length of the wetted wall is then

$$S = 2b^2 \int_0^{\pi} e^{-\tau(\eta)} \, |\cos\eta + \cos\beta| \, \sin\eta \, d\eta \tag{3.9}$$

where $\tau = \mathcal{I}m\ \omega = -\mathcal{I}m\ (\Omega^2 - \epsilon^2)^{1/2}$

The radius of curvature of the barrier is given by

$$R = \frac{ds}{d\theta} = 2b^2 e^{-\tau(\eta)} \, |\cos\eta + \cos\beta| \, \sin\eta \, \frac{d\eta}{d\theta}. \tag{3.10}$$

If X denotes the drag, Y, the lift, then it can be shown that the force is given by (e.g. Ref. 14, p. 305)

$$\begin{aligned} X + iY &= -\frac{i\rho}{2} \oint e^{i\omega} \frac{dW}{d\zeta} d\zeta \\ &= -\frac{i\rho b^2}{4} \oint \exp\left\{-i(\Omega^2 - \epsilon^2)^{1/2}\right\} (\zeta + \tfrac{1}{\zeta} + 2\cos\beta)(\zeta - \tfrac{1}{\zeta}) \frac{d\zeta}{\zeta} \end{aligned} \tag{3.11}$$

where the contour for the integral is $|\zeta| = 1$. Likewise the moment M of the force about the stagnation point C, positive in the sense of nose-down, is found to be[14]

$$M = \frac{\rho}{2} Rl \int_{(BCA)} \left[e^{-i\omega(\xi)} - e^{-i\omega(\bar{\xi})}\right] \xi \frac{dW}{d\zeta} d\zeta \ ; \tag{3.12}$$

the integration is taken around the semi-circle BCA in the ζ-plane. The above integral cannot be reduced to one on a closed contour, and, therefore, must be evaluated separately.

The above formulas are merely formal representations of various physical quantities. The magnification factor b for the physical plane may be

eliminated from Eqs. (3.8) - (3.10). If the boundary value R(s) is applied to these two resulting equations, an identity containing all the coefficients A_n in the parameter of η can be obtained. From this identity the coefficients A_n can, at least in principle, be determined. The factor b can then be expressed by (3.9) in terms of the wall length S, and in turn, X, Y, M can be calculated from Eqs. (3.11), (3.12). In practice, however, to determine the coefficients A_n from the identity would necessitate some expansion of the functions of η involved in the identity into series. This procedure leads to infinitely many transcendental equations in infinitely many unknowns. In order to obtain the general result in explicit form with sufficient accuracy, the analysis is carried out by replacing the expansion in Eq. (3.3) by the three leading terms only, that is,

$$\Omega(\zeta) = i \log\left[(1+\zeta e^{-i\beta})/(1+\zeta e^{i\beta})\right] + A_1\zeta + A_2\zeta^2 + A_3\zeta^3. \qquad (3.13)$$

If two particular points are suitably chosen on the arc ACB at which the boundary values of R and θ are applied, we get four transcendental equations from which the four unknowns, β, A_1, A_2, and A_3 can be determined, expressible in terms of the cavitation number σ, the attack angle α, and the profile shape. The rest of the physical quantities can then be calculated as shown below.

a. Lift and Drag

In the integral representing the force, given by Eq. (3.11), the integrand has inside the contour $|\zeta| = 1$ only one pole at $\zeta = 0$, but has, in addition, two branch points at $\Omega = \pm\epsilon$. Besides, the function $\Omega(\zeta)$ in the integrand has on the contour a logarithmic singularity at C and its conjugate point in the ζ-plane. Thus, if a branch cut is introduced from D to D' along the real axis in both the ζ- and Ω-planes and two other branch cuts from C to

its conjugate point outside of the unit circle in ζ-plane (see Fig. 2), the integrand is then one valued inside and on the contour in the cut plane. In practical applications, the values of the cavitation number σ usually fall in the range $0 < \sigma < 1$, corresponding to $0 < \epsilon^2 < 0.123$, which can therefore be considered small. Moreover, the modulus $|\Omega|$ is always greater than ϵ on the contour. Therefore, the exponential function in Eq. (3.11) can be expanded in terms of the small quantity ϵ^2,

$$\exp\left\{-i(\Omega^2-\epsilon^2)^{1/2}\right\} = \exp\left\{-i\Omega + \frac{i\epsilon^2}{2\Omega} + O(\epsilon^4)\right\} = e^{-i\Omega}\left(1+\frac{i\epsilon^2}{2\Omega}+O(\epsilon^4)\right). \qquad (3.14)$$

It can be verified that the term of $O(\epsilon^4)$ has indeed negligible value and thus may be omitted. Upon substitution of Eqs. (3.13), (3.14) into (3.11), the resulting integral is of the form to which the theorem of residues can readily be applied. From the residue of the integrand at $\zeta = 0$, one obtains the following result:

$$X = \pi\rho b^2\left(1+\frac{\epsilon^2}{6}\right)\left(\sin\beta + A_1/2\right)^2, \qquad (3.15)$$

$$Y = \pi\rho b^2\left(1+\epsilon^2/4\right)\left\{\left(\sin\beta\cos\beta + A_1\cos\beta + A_2/2\right)\right.$$
$$\left. + \frac{\epsilon^2}{4}\cos\beta\left(\sin\beta+\frac{A_1}{2}\right)^{-4}\left[\left(\sin\beta+\frac{A_1}{2}\right)^3 + \sin\beta\left(\sin\beta+\frac{A_1}{4}\right)\left(\frac{A_1}{2}+\frac{5}{4}A_2+A_3\right)\right]\right\}. \qquad (3.16)$$

In Eq. (3.16) the quadratic terms in A_2 and A_3 are omitted because their contribution is negligible. It should be remarked here that Eq. (3.16) is valid when the denominator, $(\sin\beta + A_1/2)$, of the last term is greater than zero, implying further that the drag X is always positive definite. For, if this quantity vanishes, then the expansion of $\Omega(\zeta)$ near $\zeta = 0$ (see Eq. (3.4)) starts with ζ^2 and hence the mapping fails to be conformal at $\zeta = 0$, indicating that the flow configuration is basically different from what is being considered. If this quantity becomes negative, then the function $\Omega(\zeta)$ changes

its branch, implying physically that the cavity shifts sides on the barrier so that different boundary conditions should be used. With the modified boundary conditions, the present formulation, however, would remain valid.

The factor b^2 in the above equation can be expressed in terms of the arc length S of the barrier. To evaluate the integral representing S in (3.9), we first expand $\exp(-\tau)$ in a way similar to that in (3.14),

$$e^{-\tau(\eta)} = \exp\left\{ \mathrm{Im}\,(\Omega^2-\epsilon^2)^{1/2} \right\} = e^{T(\eta)}\left[1 + \frac{\epsilon^2}{2}\frac{T}{\Theta^2+T^2} + O(\epsilon^4) \right] \tag{3.17}$$

where $\Omega(e^{i\eta}) = \Theta(\eta) + iT(\eta)$, and Θ, T are given in Eq. (3.5) with $A_4 = A_5 = \ldots = 0$. Substituting Eq. (3.17) into (3.9), we obtain

$$S = 2b^2 \int_0^{\pi} \left(1+\frac{\epsilon^2}{2}\frac{T}{\Theta^2+T^2}\right)\left[1+\sum_{n=1}^{3} A_n \sin n\eta\right]\left[1+\cos(\eta-\beta)\right]\sin\eta\, d\eta$$

in which the higher order terms of A_n are neglected. The function $T/(\Theta^2+T^2)$ is positive and, as can be shown, is bounded above by a constant of order unity, which depends on the value of Θ at B but is independent of ϵ. Hence the contribution from the term of $0(\epsilon^2)$ is very small relative to the first order term. Carrying out the integration, we finally obtain

$$S\,b^{-2} \equiv J = 4 + \pi\sin\beta + A_1(\pi + \tfrac{8}{3}\sin\beta) + \tfrac{\pi}{2}A_2\cos\beta - \tfrac{8}{15}A_3\sin\beta. \tag{3.18}$$

For a flat plate set at an angle α, moving at the idealized limiting condition $\sigma = 0$ ($\epsilon = 0$), the coefficients A's all vanish, as required by the condition of conformal mapping, and $\beta = \alpha$ (see Eq. (3.5b)), then Eqs. (3.15), (3.16) and (3.18) reduce to the classical result for an oblique lamina (see Ref. 15, p. 102).

b. Moment of Force; Stagnation Point; Center of Pressure

Applying a similar approximation, as described in Eq. (3.17), to Eqs.

(3.12) and (3.7), and further neglecting A_3, we obtain

$$M = 2b^2\rho\, Rl \int_0^{\pi} exp\left\{i(\beta + A_1\cos\eta + A_2\cos 2\eta)\right\}\left[\sin\beta + (A_1 + 2A_2\cos\eta)(1+\cos\beta\cos\eta)\right](\sin^2\eta)\, z(\eta)\, d\eta$$

where

$$z(\eta) = 2b^2 e^{-i\beta}\int_{\eta}^{\pi-\beta}\left[1 - iA_1 e^{i\eta} - iA_2 e^{2i\eta}\right]\left[1+\cos(\eta-\beta)\right]\sin\eta\, d\eta\,.$$

We then substitute the integral for $z(\eta)$ into the former expression, decompose accordingly the interval into two parts: $0 \le \eta \le \pi-\beta$ and $\pi-\beta \le \eta \le \pi$, and then interchange the order of integration so that the limits of integration further simplify the involved manipulation. After some tedious integrations, which are otherwise straightforward, we finally obtain

$$\begin{aligned} M/(2\pi\rho b^4) \equiv K = C_1\Big\{ &\cos\beta\left[\tfrac{5}{8} + \sin^2\beta + A_1\left(\tfrac{7}{6}\sin\beta + \tfrac{2}{3}\sin^3\beta - \tfrac{32}{45\pi}\right)\right. \\ &\left. + \frac{C_1}{2}\left(\frac{\pi}{2}-\beta\right) - A_2\left(\tfrac{3}{16}\sin\beta + \tfrac{1}{12}\sin^3\beta - \sin^5\beta + \tfrac{64}{45\pi}\right)\right\} \\ &+ C_2\left(1 + A_1 + \frac{A_2}{4}\cos\beta\right)\left(1 + \frac{128}{45\pi}\sin\beta\right) + \frac{A_2}{16}\cos\beta\left(1 + \tfrac{5}{6}A_1\right), \end{aligned} \qquad (3.19)$$

where b^2 is given by Eq. (3.18) and

$$C_1 = \sin\beta + A_1 + \frac{A_2}{2}\cos\beta\,; \qquad C_2 = \frac{1}{4}\left(A_1\cos\beta + 2A_2\right).$$

If a profile symmetrical with respect to the central chord is set with its chord normal to the free stream, then $\beta = \pi/2$ due to symmetry (see Fig. 2). Furthermore, A_2 should vanish because in this case $\Omega(\zeta)$ is necessarily an odd function of ζ (see Eq. (3.13)). It then follows from Eq. (3.19) that the moment M about the stagnation point, which is now at the central chord, vanishes as it should be expected.

Because of the indefinite location of the stagnation point, the moment of

force is usually calculated or measured referring to a fixed point. Hence, we derive here the moment M_o about the leading edge. This further requires the calculation of the position of stagnation point. Denote the distance along the wall from the stagnation point to the leading edge by S_o; then S_o can be calculated from Eq. (3.8) by letting the lower limit $\eta = \pi$. Proceeding in a manner similar to that described for the equation previous to (3.18), we obtain

$$S_o \cong 2b^2 \int_o^\beta (1 + A_1 \sin\theta - A_2 \sin 2\theta + A_3 \sin 3\theta)\,[1 - \cos(\theta+\beta)] \sin\theta\, d\theta$$

which finally leads to

$$\begin{aligned} S_o\, b^{-2} \equiv J_o = {} & 2(1-\cos\beta) + \sin\beta\,(\beta - \sin 2\beta) + A_1\left(\beta + \tfrac{4}{3}\sin\beta - \tfrac{3}{2}\sin 2\beta + \tfrac{1}{6}\sin 4\beta\right) \\ & + A_2\left(\tfrac{1}{2}\beta\cos\beta - \tfrac{1}{2}\sin\beta + \tfrac{1}{6}\sin^3\beta - 2\sin^5\beta\right) \\ & + \tfrac{2}{15} A_3 \sin\beta\left[\cos\beta\,(2 + \sin^2\beta + 24\sin^4\beta) - 2\right]. \end{aligned} \tag{3.20}$$

The factor b^2 can be eliminated by using Eq. (3.18) to give

$$\mu \equiv S_o/S = J_o/J\,. \tag{3.21}$$

Again, for a symmetric profile normal to the free stream, $\beta = \pi/2$, and $A_2 = 0$, it can be verified from Eqs. (3.18) and (3.20) that $\mu = 1/2$. For small values of β (corresponding to small α, as can be seen from Eq. (3.5b), Eq. (3.21) reduces to

$$\mu = \tfrac{17}{48}\beta^4 + O(\beta^5) \tag{3.22}$$

which shows that the stagnation point is extremely close to the leading edge for small angles of attack.

Knowing the position of the stagnation point, the moment M_o about the leading edge then becomes, for profiles of small camber,

$$M_o = M + (Y\cos\alpha + X\sin\alpha)\,S_o \tag{3.23}$$

Having obtained M_o, we can determine the location of the center of pressure, measured from the leading edge, to be approximately at

$$S_1 = M_o / (Y\cos\alpha + X\sin\alpha), \tag{3.24}$$

or, in percentage of the chord,

$$\nu = S_1/S = \mu + \frac{M}{S}(Y\cos\alpha + X\sin\alpha)^{-1}. \tag{3.25}$$

Now, consider again a symmetric profile normal to the free stream, $\alpha = \beta = \pi/2$. We have shown before that $\mu = 1/2$ and $M = 0$, hence $\nu = 1/2$. For small values of α (β is also small as previously explained), Eq. (3.22) states that μ is very small; Eq. (3.16) reduces to $Y \cong \pi\rho b^2(\beta + A_1 + A_2/2)$; Eq. (3.18) gives $S \cong 4b^2$; and $M \cong 2\pi b^4 \rho\left[\frac{5}{8}(\beta + A_1 + A_2/2) + \frac{1}{4}(A_1 + 2A_2)\right]$ from Eq. (3.19). Thus, for small α and σ, we have approximately

$$\nu \cong \frac{5}{16} + \frac{1}{8}(A_1 + 2A_2)/(\beta + A_1 + A_2/2) + O(\beta). \tag{3.26}$$

Hence the center of pressure ranges from 5/16 to 1/2 of the chord.

c. Some Basic Features of the Free Streamlines

In this section the shape of the free streamlines AD, BD' and the location of the points D and D' will now be calculated. First, we show that the assumed curvature form of the free streamlines, namely, concave towards the cavity, imposes certain conditions on the coefficients A_1, A_2 and A_3. Denote the distance along the streamline $\psi = 0$ by s, positive when away from the point C. On AD, $\zeta = -\xi$ with $1 \geq \xi \geq \xi_1$ where $-\xi_1$ is the value of ζ at D; while on BD', $\zeta = \xi$ with $1 \geq \xi \geq \xi_2$ where $\xi_2 = \zeta_{D'}$. Then the radius of curvature $R = -ds/d\theta$ on AD and $R = ds/d\theta$ on BD' should both be positive. We shall first consider R on AD. From the definition of $\Omega = \Theta + iT$ and $z(\zeta)$ (see Eqs. (3.2),(3.6)), ω and Ω are both

real on AD, and hence

$$R = -\frac{d\delta}{d\theta} = -\frac{|dz|}{d\xi}\frac{d\xi}{d\Theta}\frac{d\Theta}{d\theta} = -\frac{\theta}{\Theta}\frac{|dz|}{d\xi}\Big/\frac{d\theta}{d\xi}$$

$$= \frac{b^2}{2}\left(-\frac{\theta}{\Theta}\right)\xi^{-3}\frac{(1-\xi^2)(1-2\xi\cos\beta+\xi^2)^2}{2\sin\beta+(1-2\xi\cos\beta+\xi^2)(A_1-2A_2\xi+3A_3\xi^2)}.$$

From this equation it follows that the condition $R(\xi)\geq 0$ for $\xi \leq 1$ requires

$$2\sin\beta + (1-2\xi\cos\beta+\xi^2)(A_1-2A_2\xi+3A_3\xi^2) > 0. \tag{3.27}$$

Consequently $R(\xi)$ increases from $R(1) = 0$ as ξ decreases from 1. A similar requirement for positive R on BD' is, for $\xi_2 \leq \xi \leq 1$,

$$2\sin\beta + (1+2\xi\cos\beta+\xi^2)(A_1+2A_2\xi+3A_3\xi^2) > 0. \tag{3.28}$$

It will be only stated here that these two subsidiary conditions are in general satisfied owing to the facts that the coefficient of the first term in Eq. (3.4) is positive and that A_n's decrease rapidly with respect to A_1. However, no further elaboration will be made here on these points.

A parametric representation $x(\xi)$, $y(\xi)$ of the free streamline AD can be obtained by integrating Eq. (3.6) along $\zeta = -\xi$ from $\xi = 1$ to $\xi \geq \xi_1$. On AD, $\tau = \mathrm{Im}\,\omega = 0$, and hence, referring to the point A, we have

$$x - x_A = -\frac{S}{2J}\int_1^{\xi} \xi^{-3}(1-2\xi\cos\beta+\xi^2)(1-\xi^2)\cos\theta\, d\xi, \tag{3.29}$$

$$y - y_A = -\frac{S}{2J}\int_1^{\xi} \xi^{-3}(1-2\xi\cos\beta+\xi^2)(1-\xi^2)\sin\theta\, d\xi. \tag{3.30}$$

In the above equations $\cos\theta$ and $\sin\theta$ are complicated functions of ξ,

$$\theta = -(\Theta^2-\epsilon^2)^{1/2}, \tag{3.31}$$

$$\Theta = -2\tan^{-1}\frac{\xi\sin\beta}{1-\xi\cos\beta} - A_1\xi + A_2\xi^2 - A_3\xi^3. \tag{3.32}$$

To simplify the calculation, we approximate Eq. (3.31) by $\theta = -(\Theta + \epsilon)$ on AD, which should be good for θ both small and large. Then we obtain the following approximate formulas

$$\cos\theta = (1-2\xi\cos\beta+\xi^2\cos 2\beta)/(1-2\xi\cos\beta+\xi^2),$$

$$\sin\theta = \frac{2\xi(1-\xi\cos\beta)\sin\beta + (A_1\xi - A_2\xi^2 - \epsilon)(1-2\xi\cos\beta+\xi^2\cos 2\beta)}{1-2\xi\cos\beta+\xi^2}.$$

Substituting these values into Eqs. (3.29), (3.30) and carrying out the integrations, we finally obtain

$$2J(x-x_A)/S \cong \tfrac{1}{2}(1-\xi^2)(\xi^{-2}-\cos 2\beta) - 2\cos\beta(1-\xi)^2\xi^{-1} + 2\sin^2\beta\log\xi; \tag{3.33}$$

$$\begin{aligned} 2J(y-y_A)/S \cong\ & (2\sin\beta + A_1 + 2\epsilon\cos\beta)(1-\xi)^2/\xi - \epsilon\left(\frac{1-\xi^2}{2\xi^2} + \log\xi\right) \\ & + (\sin 2\beta + 2A_1\cos\beta + A_2 + \epsilon\cos 2\beta)[\log\xi + \tfrac{1}{2}(1-\xi^2)] \\ & + \tfrac{1}{3}(A_1\cos 2\beta + 2A_2\cos\beta)(1-\xi)^2(2+\xi) - \frac{A_2}{4}(1-\xi^2)^2\cos 2\beta. \end{aligned} \tag{3.34}$$

To find the location of D, (x_D, y_D), we first determine the value ξ_1 corresponding to $\Omega = +\epsilon$. Then, by letting $\Omega = -\epsilon$ and $\zeta = -\xi_1$ in Eq. (3.4), we obtain

$$\xi_1 = \frac{\epsilon}{a_1}\left[1 + \frac{a_2\epsilon}{a_1^2} + O(\epsilon^2)\right].$$

Using this value of ξ_1, one can easily derive from Eqs. (3.33), (3.34) that

$$x_D \cong \frac{S}{J}\left\{\frac{a_1^2}{4\epsilon^2} + O(\frac{1}{\epsilon})\right\} = \frac{S}{J}\left(\frac{2\sin\beta + A_1}{\sigma}\right)^2\left[1 + O(\sigma)\right], \tag{3.35}$$

$$y_D \cong \frac{S}{J}\left\{\frac{a_1^2}{2\epsilon} + O(\log\epsilon)\right\} = \frac{S}{J}\,\frac{(2\sin\beta + A_1)^2}{\sigma}\left[1 + O(\sigma\log\sigma)\right]. \qquad (3.36)$$

The above value of x_D and y_D may be regarded respectively as the half-length and half-width of the cavity. Thus we see that for σ small the cavity length is proportional to σ^{-2}, while the cavity width, proportional to σ^{-1}. It may also be seen that the free streamline near D lies close to a parabola

$$y^2/x \cong a_1^2\, S/J = b^2(2\sin\beta + A_1)^2 \equiv C, \qquad \text{say.}$$

Then a comparison with Eq. (3.15) shows that the drag X can be expressed by

$$X \cong \pi\rho b^2(\sin\beta + A_1/2)^2 = \pi\rho C/4$$

which is the general formula of Levi-Civita.[16]

Now, in order to determine these unknown coefficients A_1, A_2, A_3 and β and thus to exhibit explicitly the effects of cavitation number σ, the attack angle α and the profile geometry, two specific examples, the circular arc and the flat plate, will be worked out below.

IV. CAVITATING HYDROFOILS WITH CIRCULAR ARC AND FLAT PLATE PROFILE

Let us first consider the hydrofoil having the circular arc profile, with radius R and arc angle 2γ (see Fig. 3). The flat plate is just a special case with $\gamma \to 0$ $(R \to \infty)$. We shall here restrict ourselves to small values of γ, say, $\gamma < \pi/4$. The arc length S and the length ℓ of the chord AB are then

$$S = 2\gamma R\ ; \qquad \ell = 2R\sin\gamma = 2\gamma R(1 - \gamma^2/6). \qquad (4.1)$$

Now we choose the end points A and B to which the following boundary conditions are applied:

$$\text{(i)}\ \theta_A = \pi - \alpha + \gamma\ , \qquad \text{(ii)}\ \theta_B = -\alpha - \gamma\ , \tag{4.2}$$

$$\text{(iii), (iv) radius of curvature at A and B} = R = \frac{S}{2\gamma}\ .$$

These four conditions enable us to determine A_1, A_2, A_3 and β which in turn can be used to check the radius of curvature at other points on the boundary. Applying (i) and (ii) to the definition of Θ (see Eqs. (3.2), (3.5)), we obtain

$$\Theta_B = (\theta_B^2 + \epsilon^2)^{1/2} = \left[(\alpha+\gamma)^2 + \epsilon^2\right]^{1/2} = \beta + A_1 + A_2 + A_3\ ,$$

$$\Theta_A = -(\theta_A^2 + \epsilon^2)^{1/2} = -\pi + \alpha - \gamma - \tfrac{1}{2}\epsilon^2/\theta_A = -\pi + \beta - A_1 + A_2 - A_3\ .$$

In the second equation the value with 1/2 power is expanded for θ_A is always much greater than ϵ, but in the first equation no expansion is made because the ratio ϵ/θ_B may not be small. Adding and subtracting these two equations, we have

$$A_1 + A_3 = \gamma + \frac{1}{2}\left\{\left[(\alpha+\gamma)^2 + \epsilon^2\right]^{1/2} - (\alpha+\gamma)\right\} + \frac{\epsilon^2}{4}(\pi - \alpha + \gamma)^{-1}\ , \tag{4.3}$$

$$\beta + A_2 = \alpha + \frac{1}{2}\left\{\left[(\alpha+\gamma)^2 + \epsilon^2\right]^{1/2} - (\alpha+\gamma)\right\} - \frac{\epsilon^2}{4}(\pi - \alpha + \gamma)^{-1}\ . \tag{4.4}$$

In applying the conditions (iii), (iv), we first note that at B, $\tau = 0$ and

$$\frac{d\theta}{d\eta} = \frac{(\theta_B^2 + \epsilon^2)^{1/2}}{\theta_B}\frac{d\Theta}{d\eta} \longrightarrow -\frac{(\theta_B^2 + \epsilon^2)^{1/2}}{\theta_B}(A_1 + 4A_2 + 9A_3)\sin\eta\ , \quad \text{as}\ \ \eta \to 0.$$

Hence, from Eq. (3.10)

$$-\frac{\theta_B(1+\cos\beta)}{(\theta_B^2+\epsilon^2)^{1/2}}\left(A_1+4A_2+9A_3\right)^{-1}=\frac{R}{2b^2}=\frac{RJ}{2S}=\frac{J}{4\gamma};$$

or,

$$A_1+4A_2+9A_3=(4\gamma/J)(\alpha+\gamma)\left[(\alpha+\gamma)^2+\epsilon^2\right]^{-1/2}(1+\cos\beta). \tag{4.5}$$

Similarly, application of the boundary condition (iv) at A yields

$$A_1-4A_2+9A_3=(4\gamma/J)(1-\cos\beta)\left[1+O(\epsilon^2)\right]. \tag{4.6}$$

In Eqs. (4.5) and (4.6), J, as defined by Eq. (3.18), also contains A_1, A_2, A_3 and β. Thus Eqs. (4.3)-(4.6) together with (3.18) represent five transcendental equations for five unknowns A_1, A_2, A_3, β and J. The solution, however, can easily be approximated with good accuracy by using an iteration procedure. For the present purpose, the following approximation is sufficient

$$\beta=\alpha+\frac{1}{2}\delta-\frac{\epsilon^2}{4(\pi-\alpha+\gamma)}-\frac{\gamma}{4+\pi\sin\alpha}\left\{\frac{\alpha+\gamma}{\left[(\alpha+\gamma)^2+\epsilon^2\right]^{1/2}}\cos^2\frac{\alpha}{2}-\sin^2\frac{\alpha}{2}\right\}, \tag{4.7a}$$

$$\delta=\left[(\alpha+\gamma)^2+\epsilon^2\right]^{1/2}-(\alpha+\gamma); \tag{4.7b}$$

$$A_1=\gamma\left\{1+\frac{\pi\sin\alpha}{8(4+\pi\sin\alpha)}\right\}+\frac{9}{16}\delta\left\{1+\frac{\gamma(1+\cos\alpha)}{9\left[(\alpha+\gamma)^2+\epsilon^2\right]^{1/2}}\right\}+\frac{9\epsilon^2}{32(\pi-\alpha+\gamma)}; \tag{4.8}$$

$$A_2=\frac{\gamma}{4+\pi(A_1+\sin\beta)}\left\{\frac{\alpha+\gamma}{\left[(\alpha+\gamma)^2+\epsilon^2\right]^{1/2}}\cos^2\frac{\beta}{2}-\sin^2\frac{\beta}{2}\right\}; \tag{4.9}$$

$$A_3=\frac{1}{9}(\gamma-A_1)-\frac{\gamma}{9(4+\pi\sin\alpha)}\left\{\pi\sin\beta+\frac{2\delta(1+\cos\alpha)}{\left[(\alpha+\gamma)^2+\epsilon^2\right]^{1/2}}\right\}; \tag{4.10}$$

whereas J is still given by (3.18). The above result shows that $(\beta-\alpha)$, A_1, A_2 and A_3 are all of $O(\gamma, \epsilon^2)$ for all α; and in particular, $(\beta-\alpha)$, A_2 and A_3 reduce to $O(\gamma\epsilon^2, \epsilon^4)$ for α close to $\pi/2$. Moreover, the fact that A_3

is much smaller than A_1 indicates a good accuracy of the expansion given by Eq. (3.13). If the above quantities are used to check the curvature and slope of the solid boundary at some other points, say at $\zeta = e^{i\pi/2}$, one can easily find that the agreement is within a factor at most of $0(\gamma, \epsilon^2)$. It should also be remarked here that if more terms were taken in the expansion (3.13), then the first three coefficients A_1, A_2, A_3 would differ slightly from the above value (4.8-4.10). However, it can be verified that the "improvement" of the solution by taking terms more than three is actually unappreciable.

Now we define the conventional drag coefficient, lift coefficient and moment coefficient (about the leading edge) as follows:

$$X = \frac{1}{2}\rho U^2 \ell\, C_D\,; \qquad Y = \frac{1}{2}\rho U^2 \ell\, C_L\,; \qquad M_0 = \frac{1}{2}\rho U^2 \ell^2 C_{M_0}\,. \tag{4.11}$$

Then, for γ not too large ($< \pi/4$), we compile some of the previous results and note that $U = (1+\sigma)^{-1/2}$, we finally obtain:

$$C_D = \frac{2\pi}{J}\left(1+\sigma+\frac{\epsilon^2}{6}+\frac{\gamma^2}{6}\right)\left[\sin\beta + \frac{A_1}{2}\right]^2; \tag{4.12}$$

$$C_L = \frac{2\pi}{J}\left(1+\sigma+\frac{\epsilon^2}{4}+\frac{\gamma^2}{6}\right)\left\{\left[\sin\beta\cos\beta + A_1\cos\beta + \frac{A_2}{2}\right]\right.$$

$$\left. + \frac{\epsilon^2}{4}\frac{\cos\beta}{(\sin\beta + A_1/2)^4}\left[\left(\sin\beta+\frac{A_1}{2}\right)^3 + \sin\beta\left(\sin\beta+\frac{A_1}{4}\right)\left(\frac{A_1}{2}+\frac{5}{4}A_2+A_3\right)\right]\right\}; \tag{4.13}$$

$$C_{M_0} = \frac{4\pi}{J^2}\left(1+\sigma+\frac{\gamma^2}{3}\right)K + \mu\left(C_L\cos\alpha + C_D\sin\alpha\right) \tag{4.14}$$

where β, A_1, A_2, A_3 are given by Eqs. (4.7)-(4.10); J is given by (3.18); K, by (3.19); μ, by (3.20), (3.21) and $\epsilon = 1/2\log(1+\sigma)$.

The results for the flat plate hydrofoil can be deduced from the above expressions by putting $\gamma = 0$. For the circular arc hydrofoil with its convex

side toward the approaching stream at positive α (see Fig. 4a), the above formulas still hold if γ assumes a negative value. For flow configurations with positive γ but negative α (see Fig. 4b), the results are that C_D stays the same, but C_L and C_M have oppositive signs as those of flow case (4a).

There are however, several points of complication at which the above results may become invalid, and thus should be applied with great care. First, there in general exists a certain small α, say, α_p, positive or negative, at which the free streamline AD given by Eqs. (3.33), (3.34) would cut into the solid boundary. It could be conjectured that a partial cavitation, that is, with the rear end of the cavity reattached to the boundary, probably is established for α around α_p. The present theory certainly does not cover partially cavitating flows. Second, there is another critical value of α, say, $\alpha_c(\gamma,\sigma)$ at which $\beta = 0$, implying that the stagnation point is then at the leading edge. Hence the cavity will shift side on the boundary for $\alpha < \alpha_c$. The value of α_c is in general less than α_p. Third, in flow configurations shown in Fig. 4, the streamline will be in a more critical position at B than at A. In other words, the flow is more likely to separate in front of B for small enough α; and thus a rear part of the boundary will be inside the full cavity. This critical condition will take place when either the slope or the radius of curvature of streamline BD' at B is numerically greater than that of the solid boundary at B. These points will be touched upon in the following explicit calculations, though the clarification of these points requires further study.

a. Inclined Flat Plate

For an inclined flat plate, $\gamma = 0$, and hence Eqs. (4.7)-(4.10) reduce to

$$\beta = \alpha + \frac{1}{2}\left[(\alpha^2+\epsilon^2)^{1/2} - \alpha\right] - \frac{1}{4}\epsilon^2/(\pi-\alpha), \tag{4.15}$$

$$A_1 = \frac{9}{16}\left[(\alpha^2+\epsilon^2)^{1/2}-\alpha\right] + \frac{9}{32}\epsilon^2/(\pi-\alpha)\,, \qquad A_2 = 0\,, \qquad A_3 = -\frac{1}{9}A_1 \tag{4.16}$$

and

$$J = 4 + \pi\sin\beta + A_1(\pi + 2.72\sin\beta). \tag{4.17}$$

The expressions for C_L and C_D then can be simplified to:

$$C_D \cong \frac{2\pi}{J}\left(1+\sigma+\frac{\epsilon^2}{6}\right)\left[\sin\beta + \frac{A_1}{2}\right]^2, \tag{4.18}$$

$$C_L \cong \frac{2\pi}{J}\left(1+\sigma+\frac{\epsilon^2}{4}\right)\cos\beta\left[(\sin\beta+A_1)+\frac{\epsilon^2}{32}\,\frac{8\sin\beta(\sin\beta+A_1)^2 + A_1^2(A_1-\sin\beta)}{(\sin\beta+A_1/2)^4}\right]. \tag{4.19}$$

In the idealized case of $\sigma = 0$ (hence $\epsilon = 0$), $\beta = \alpha$ and A_1, A_2, A_3 all vanish, the above result then reduces to Rayleigh's theory of the oblique lamina (e.g. ref. 15, p. 102):

$$C_D = \frac{2\pi\sin^2\alpha}{4+\pi\sin\alpha}\,; \qquad C_L = C_D\cot\alpha. \tag{4.20}$$

When $\alpha = \pi/2$ but $\sigma > 0$, Eqs. (4.17)-(4.19) become

$$C_D \cong \frac{2\pi}{4+\pi}\left(1+\sigma+0.05\sigma^2\right), \qquad C_L = 0. \tag{4.21}$$

which are well-known results (see also Eq. (2.2)).

For general values of α and σ, one more physical requirement, however, should be pointed out. For a fully cavitating flow past the oblique flat plate, the local pressure is everywhere normal to the plate and, besides, there is no singular force at leading edge as in the noncavitating case. Consequently C_L and C_D should satisfy the condition

$$C_D/C_L = \tan\alpha \qquad \text{for all } \alpha \text{ and } \sigma. \tag{4.22}$$

In the special cases (i) $\sigma = 0$, (ii) α close to $\pi/2$ and $\sigma > 0$, the above condition is obviously satisfied (see Eqs. (4.20), (4.21)). However, in the general case, it is rather difficult to derive this relation from Eqs. (4.18), (4.19), because of the complicated manner in which the dependence on α and σ appears. Under this circumstance, the condition (4.22) can only be used as a check in numerical computation to assure the correctness of this theory.

Another approximate formula for C_L, when α is small but σ is left arbitrary, has been given by Betz. The main idea is first to linearize the Rayleigh's formula (4.20) to obtain $\pi\alpha/2$ and then by adding to this quantity the pressure coefficient on the upper suction side, namely, σ, to obtain

$$C_L = \frac{\pi}{2}\alpha + \sigma. \tag{4.23}$$

This approximation appears, in general, too rough.

On the other hand, as σ increases the cavity dimension diminishes (see Eqs. (3.37), (3.38)); in some cases it is observed experimentally that the cavity collapses completely for σ approximately greater than 1.5. In the latter flow condition C_L and C_D then resume their noncavitating (aerodynamic) values:

$$C_L \cong 2\pi \sin\alpha, \qquad C_D \cong (2\cos\alpha)\, C_f \tag{4.24}$$

where C_f is the mean friction coefficient on one side of the plate.

The value of C_L given by (4.19) is plotted against α for different values of σ in Figs. 5 and 6. The aerodynamic value of C_L given by (4.24) is also shown for comparison. For a given value of σ, there is a certain small α, say, α_p at which the cavitating value of C_L becomes equal to the aerodynamic value if the fully cavitating model is assumed still possible

(e.g. $\alpha_p = 4.5^\circ$ for $\sigma = 0.4$). A further extrapolation (dotted lines) of Eq. (4.19), without justification, to smaller α would yield an implausible result that the cavitating value of C_L would be greater than its corresponding aerodynamic value. As a physical conjecture, this result is unacceptable. Instead, we expect that near $\alpha = \alpha_p$ partially cavitating flow takes place, a transitional stage between the fully cavitating and fully wetted conditions. This argument is supported by experimental evidence, as shown by the double-dotted lines in Figs. 5 and 6. Thus, the aerodynamic value of C_L for a fully wetted hydrofoil is actually the asymptote to which the cavitating C_L at every σ approaches from below as α decreases from α_p.

The value of C_D given by Eq. (4.18) is similarly plotted in Figs. 7 and 8. In the cavitating range of practical interest, the Reynolds number of the flow is in general very large, say, of the order 5×10^5 or greater. Then the frictional drag coefficient C_f, as can be estimated by using the Prandtl-Schlichting formula (e.g. ref. 17, p. 33), is of the order 0.005 which is much smaller than the cavity C_D for almost all α and σ and can thus be neglected.

A series of experiments[18] was carried out in the Hydrodynamics Laboratory, California Institute of Technology, at about the same time the present theoretical result was obtained. In order to compare the theory with the experiments, C_L and C_D are further cross-plotted against σ in Figs. 9 and 10 in which the experimental data are also shown.* The agreement is very good. As a further check, the value C_L/C_D is plotted against α for several σ and is compared with $\cot\alpha$ in Fig. 11. The deviation is less than a few

---

*In these experimental data, the correction due to tunnel-wall effect was not taken into account. However, the cavitation number σ was computed based on the measured cavity pressure which presumably absorbs a part of the wall-effect correction. For the detailed description, refer to Ref. 18).

percent, implying the accuracy of the present theory.

Some of the salient points of the previous results may be summarized here.

(i) The results plotted in Figs. 9 and 10 show that for α large, say, greater than 45°, the values of C_L and C_D approach respectively the asymptotes

$$C_L(\sigma,\alpha) = (1+\sigma)\,C_L(0,\alpha), \qquad C_D(\sigma,\alpha) = (1+\sigma)\,C_D(0,\alpha), \tag{4.25}$$

which are shown as dotted lines. For α small, they deviate appreciably from these asymptotes; the deviation is much more marked for C_L since here the deviation of C_D is magnified by a factor $\cot\alpha$. For instance, the slope $dC_L/d\sigma$ becomes greater than unity for $\alpha < 15^{\circ}$ and $\sigma > 0.2$.

(ii) It is to be noted from Figs. 5 and 6 that, after the hydrofoil at small α is fully cavitated, $dC_L/d\alpha$ decreases to values much smaller than that of fully wetted case, which is approximately equal to 2π. This means that fully cavitating hydrofoils are quite insensitive to variations of attack angle α. However, the drag coefficient is relatively more sensitive due to the relation (4.22). Differentiating Eq. (4.22) with respect to α, we have

$$\frac{1}{C_D}\frac{dC_D}{d\alpha} = \frac{1}{C_L}\frac{dC_L}{d\alpha} + 2\csc 2\alpha. \tag{4.26}$$

Thus, the percentagewise change of C_D is always greater than that of C_L.

The location of the stagnation point, $\mu = S_o/S$, as given by Eqs. (3.18) and (3.20), is plotted in Fig. 12 for this oblique flat plate by using the quantities given in Eqs. (4.15)-(4.17). It is of interest to note that σ has really negligible effect on μ. With the aid of Figs. 9, 10 and 12, the moment coefficient C_{M_o} about the leading edge of the flat plate (see Eq. (4.14) with $\gamma = 0$) is

further computed and plotted against σ in Fig. 13. The theoretical value of C_{M_0} is also in fair agreement with the experimental data.[18] From these results the location of the center of pressure

$$\nu = C_{M_0} / (C_L \cos\alpha + C_D \sin\alpha) \tag{4.27}$$

can be easily deduced. The result shows that ν, like μ, is also independent of σ for all practical range of σ (see Fig. 12). It varies almost linearly from one-third chord at small α to half-chord at $\alpha = \pi/2$.

The location of the free streamlines, as given by Eqs. (3.33), (3.34), is computed and plotted for $\alpha = 10^{\circ}$ in Fig. 14.

b. An Example of Circular Arc Hydrofoils; Further Discussions

With a knowledge of some essential hydrodynamic features of the flat plate hydrofoil, we may further note several general characteristics of the camber effect in cavity flows by examining the circular arc profile.

First, when both γ and ϵ are assumed to be small, then at $\alpha = \pi/2$, we have

$$A_1 \cong \gamma + \frac{9}{8\pi}\epsilon^2, \qquad A_3 \cong -\frac{\epsilon^2}{8\pi} - 0.05\gamma, \qquad A_2 \text{ and } (\beta-\alpha) = O(\gamma\epsilon^2);$$

and hence

$$C_D \cong \frac{2\pi}{4+\pi}(1+\sigma)\left[1 + \frac{4\gamma}{3(4+\pi)}\right], \qquad C_L = 0. \tag{4.28a}$$

Therefore

$$\left(\frac{dC_D}{d\gamma}\right)_{\alpha=\pi/2} \cong \frac{8\pi}{3(4+\pi)^2}(1+\sigma) \cong \frac{1}{6}(1+\sigma). \tag{4.28b}$$

These equations then represent the effect of camber on pure drag problems.

Second, in order to exhibit the effect of camber on C_L and C_D for all α, we consider the limiting case $\epsilon \to 0$ and $\gamma \to 0$, in which case

$$\frac{dA_1}{d\gamma} \to 1, \qquad \frac{dA_2}{d\gamma} = -\frac{d\beta}{d\gamma} \to \frac{\cos\alpha}{4+\pi\sin\alpha}.$$

It then follows from Eqs. (4.12), (4.13) that as $\epsilon \to 0$, $\gamma \to 0$,

$$\frac{dC_L}{d\gamma} \cong \frac{7\pi\cos\alpha}{(4+\pi\sin\alpha)^2}\left\{1+\frac{16}{21}\sin\alpha+\frac{4}{7}\sin^2\alpha\right\}; \tag{4.29}$$

$$\frac{dC_D}{d\gamma} \cong \frac{4\pi\sin\alpha}{(4+\pi\sin\alpha)^2}\left\{1-\frac{1}{3}\sin^2\alpha+\frac{\pi\sin\alpha\cos^2\alpha}{4(4+\pi\sin\alpha)}\right\}. \tag{4.30}$$

Therefore,

$$\frac{dC_L}{d\gamma} \to \frac{7\pi}{16}, \quad \frac{dC_D}{d\gamma} \to 0 \qquad \text{as} \quad \alpha \to 0,\ \gamma \to 0 \ \text{and} \ \epsilon \to 0, \tag{4.31}$$

$$\frac{dC_D}{d\gamma} \to \frac{8\pi}{3(4+\pi)^2}, \quad \frac{dC_L}{d\gamma} \to 0 \qquad \text{as} \quad \alpha \to \frac{\pi}{2},\ \gamma \to 0 \ \text{and} \ \epsilon \to 0. \tag{4.32}$$

This result shows that for small α positive camber is very favorable for increasing C_L with negligible effect on C_D. On the other hand, when σ is so large that the hydrofoil is fully wetted, then we obtain the well-known aerodynamic value of C_L :

$$C_L = 2\pi\sin\left(\alpha+\frac{\gamma}{2}\right), \tag{4.33}$$

from which we derive

$$\left(\frac{dC_L}{d\gamma}\right)_{\alpha\to 0,\,\gamma\to 0} = \pi. \tag{4.34}$$

Although the value of $dC_L/d\gamma$ for fully cavitated hydrofoil is less than that in fully wetted flow, a comparison, however, can be made on a different basis. If we compare these values at the same effective angle of attack (aerodynamic)

$$\alpha_e = \alpha + \frac{\gamma}{2},$$

then the aerodynamic value of C_L is almost the same for same α_e, but the cavitated value of C_L still increases with increase in γ, holding α_e fixed. The rate of increase in this case can be estimated to be $dC_L/d\gamma = 1/2$ at equal α_e. The influence of γ on C_L and C_D at $\sigma = 0$ is shown in Figs. 15 and 16 for two particular values of γ, 4° and 8°.

Rosenhead proposed an empirical formula for small cambers at $\sigma = 0$ as follows:[2]

$$C_P = \frac{2\pi \sin\alpha}{4+\pi\sin\alpha} + \frac{20\pi}{9}\,\frac{2+\cos\alpha+3\cos^2\alpha}{(4+\pi\sin\alpha)^2}\tan\frac{\gamma}{2} \tag{4.35a}$$

and

$$C_L = C_P \cos\delta, \qquad C_D = C_P \sin\delta \tag{4.35b}$$

where the angle δ can be computed according to Rosenhead's formulation. The value of δ is in general very close to α. Equation (4.35) is plotted in Fig. 15 for several points with $\gamma = 8^\circ$. The result shows that this formula is in good agreement with the present theory for α small.

Finally, we present here some explicit results of a numerical example with $\gamma = 8^\circ$ to show the over-all effects due to σ, α and γ. Since both $C_L(\sigma, \gamma, \alpha)$ and $C_D(\sigma, \gamma, \alpha)$ approach their asymptotes $(1+\sigma)\,C_L(0, \gamma, \alpha)$ and $(1+\sigma)C_D(0, \gamma, \alpha)$ for α large, the calculation is limited here to $\alpha \leq 30^\circ$. For $10^\circ < \alpha < 30^\circ$, the calculated values of C_L and C_D are plotted against σ in Figs. 17 and 18 together with some experimental data.[18] The agreement here may also be considered as good.

ACKNOWLEDGMENTS

The author wishes to express his great appreciation for many useful discussions with Professors M. S. Plesset and H. S. Tsien. He also wishes to thank Dr. B. R. Parkin for his interest in planning an experimental program in order to check the present theory, and for his courtesy in furnishing the data used here. He also thanks Miss Z. Lindberg for her help in numerical computations.

REFERENCES

1. Poole, E.G.C., "On the Discontinuous Motion Produced in an Infinite Stream by Two Plate Obstacles", Proc. London Math. Soc., Vol. 22 (2), p. 425, 1924.

2. Rosenhead, L., "Resistance to a Barrier in the Shape of an Arc of a Circle", Proc. Roy. Soc. (A), Vol. 117, p. 417, 1928.

3. Gilbarg, D. and Serrin, J., "Free Boundaries and Jets in the Theory of Cavitation", J. of Math. and Phys., Vol. 29, No. 1, 1950.

4. Riabouchinsky, D., "On Steady Fluid Motions with Free Surfaces", Proc. London Math. Soc., Vol. 19 (2), p. 206, 1921.

5. Kreisel, G., "Cavitation with Finite Cavitation Numbers", Admiralty Research Laboratory Report, No. R1/H/36, Jan. 1946.

6. Roshko, A., "A New Hodograph for Free-Streamline Theory", NACA TN 3168, July 1954.

7. Eppler, R., "Beiträge zu Theorie und Anwendung der unstetigen Strömungen", Journal of Rational Mechanics and Analysis, Vol. 3, No. 5, p. 591, 1954.

8. Gurevich, M., "Some Remarks on Stationary Schemes for Cavitation Flow about a Flat Plate", David Taylor Model Basin Translation No. 224, 1948.

9. Gilbarg, D. and Rock, H.H., "On Two Theories of Plane Potential Flows with Finite Cavities", Naval Ordnance Laboratory, Memorandum 8718, August 1946.

10. Goldstein, S., "Modern Developments in Fluid Mechanics", Oxford Press, 1950.

11. Fage, A. and Johansen, F.C., "On the Flow of Air Behind an Inclined Flat Plate of Infinite Span", R and M No. 1104, British A.R.C., 1927.

12. Plesset, M.S. and Perry, B., "On the Application of Free Streamline Theory to Cavity Flows", Extrait des Mémoires sur la Mécanique des Fluides, offerts à M.D. Riabouchinsky a l'occasion de son Jubilé Scientifique, Ministere de l'Air, 1954.

13. Reichardt, H., "The Laws of Cavitation Bubbles at Axially Symmetrical Bodies in a Flow", MAP Reports and Translations No. 766, 1946.

14. Milne-Thomson, L.M., "Theoretical Hydrodynamics", MacMillan Co., 1949.

15. Lamb, H., "Hydrodynamics", Dover Publications, New York, 1945.

16. Levi-Civita, T.,"Scie e leggi de resistenzia", Rend. Cir. Mat. Palermo, 23, p. 1, 1907.

17. Schlichting, H., "Boundary Layer Theory", NACA TM No. 1218, 1949.

18. Parkin, B.R., "Experiments on Circular Arc and Flat Plate Hydrofoils in Noncavitating and in Full Cavity Flow, California Institute of Technology, Hydrodynamics Laboratory Report (in preparation).

PHYSICAL PLANE HODOGRAPH PLANE

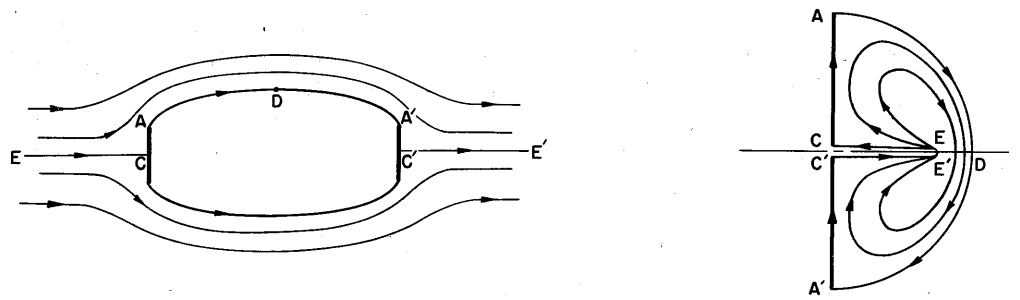

(a) RIABOUCHINSKY'S IMAGE MODEL

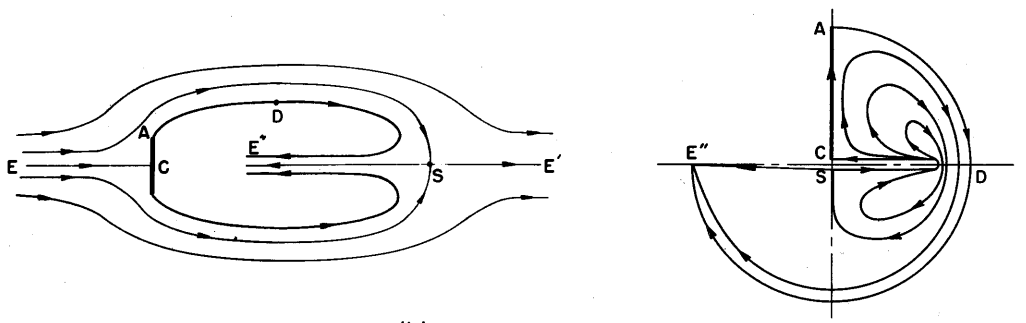

(b) REENTRANT JET MODEL

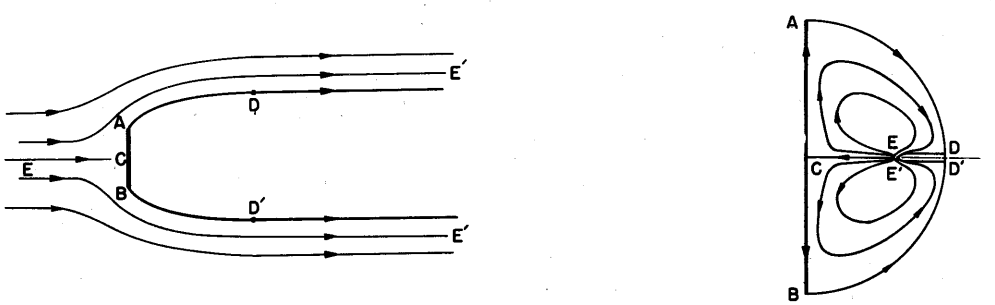

(c) ROSHKO'S DISSIPATION MODEL

Fig. 1 - Flows in the physical and hodograph plane for the various models. Note the resemblance of the streamlines in the hodograph planes near the plate AC.

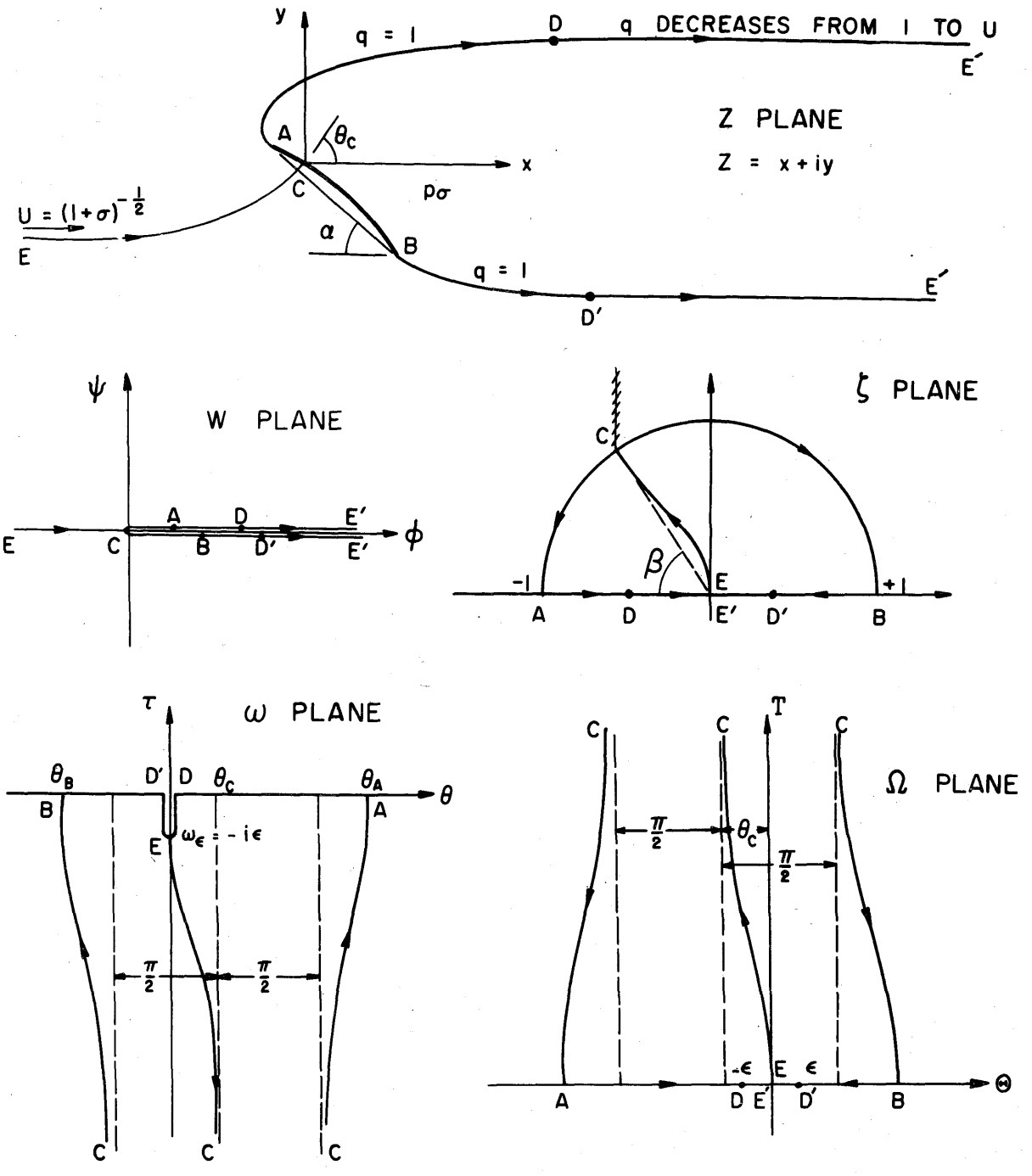
y
q = 1
D
q DECREASES FROM 1 TO U
E'
Z PLANE
Z = x + iy
A
θc
x
C
pσ
U = (1+σ)^-½
α
B
E
q = 1
E'
D'
ψ
W PLANE
A
D
E'
E
C
B
D'
E'
φ
ζ PLANE
C
β
-1
E
+1
A
D
E'
D'
B
τ
ω PLANE
θB
D'
D
θc
θA
θ
B
A
E
ωε = - iε
π/2
π/2
C
C
C
T
C
C
C
Ω PLANE
π/2
θc
π/2
-ε
E
ε
Θ
A
D
E'
D'
B

Fig. 2

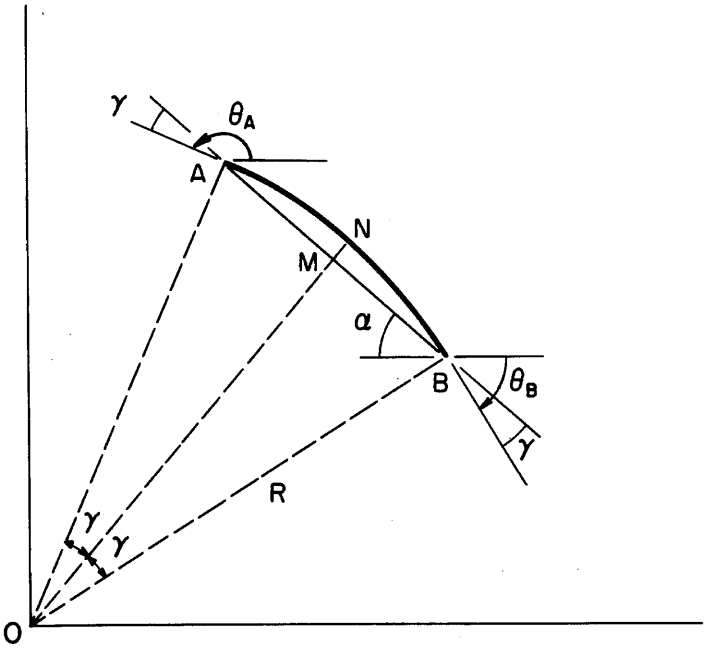

Fig. 3 - The circular arc profile.

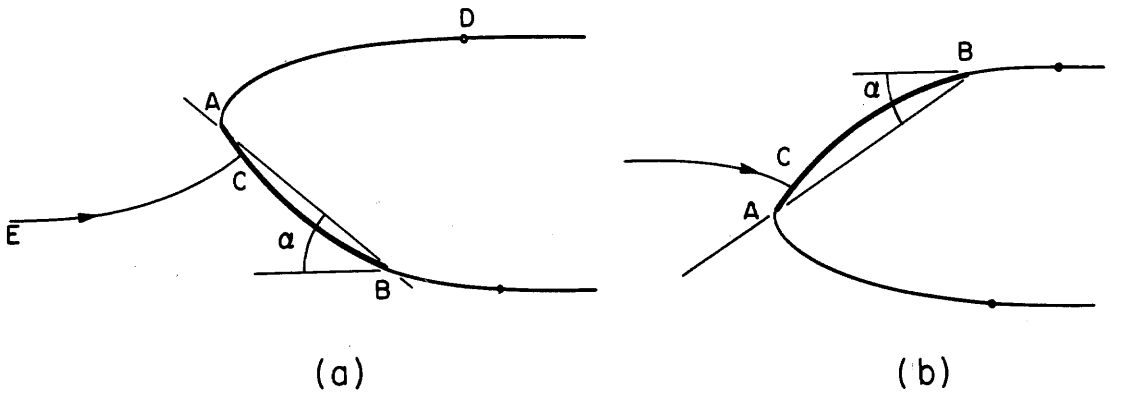

Fig. 4

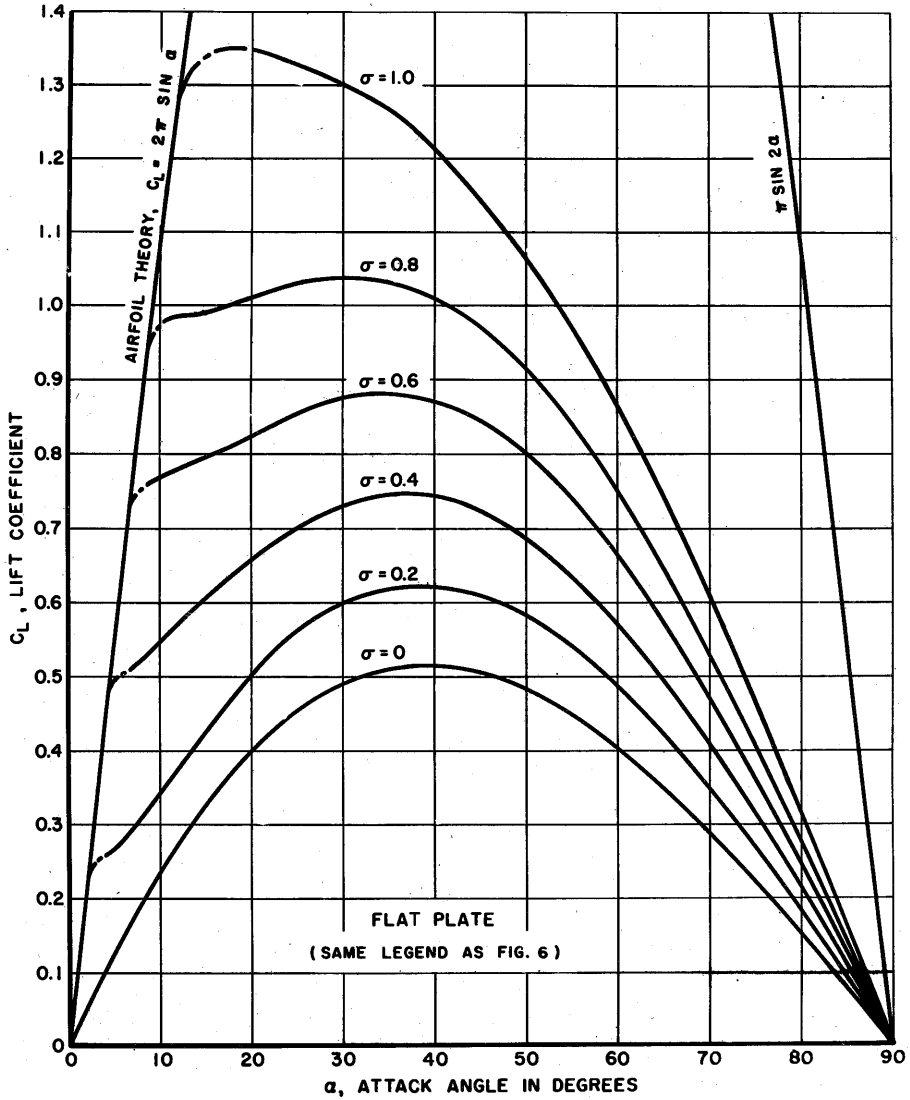

Fig. 5 - The dependence of C_L on α.

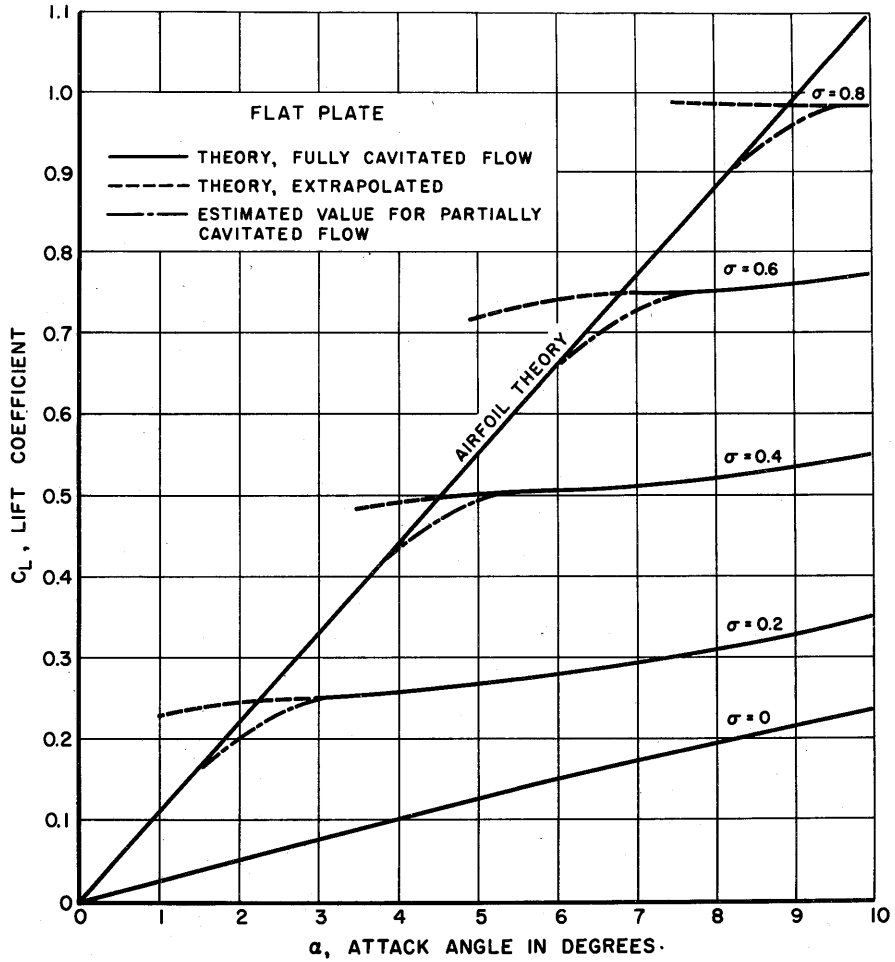

Fig. 6 - Values of C_L for small α.

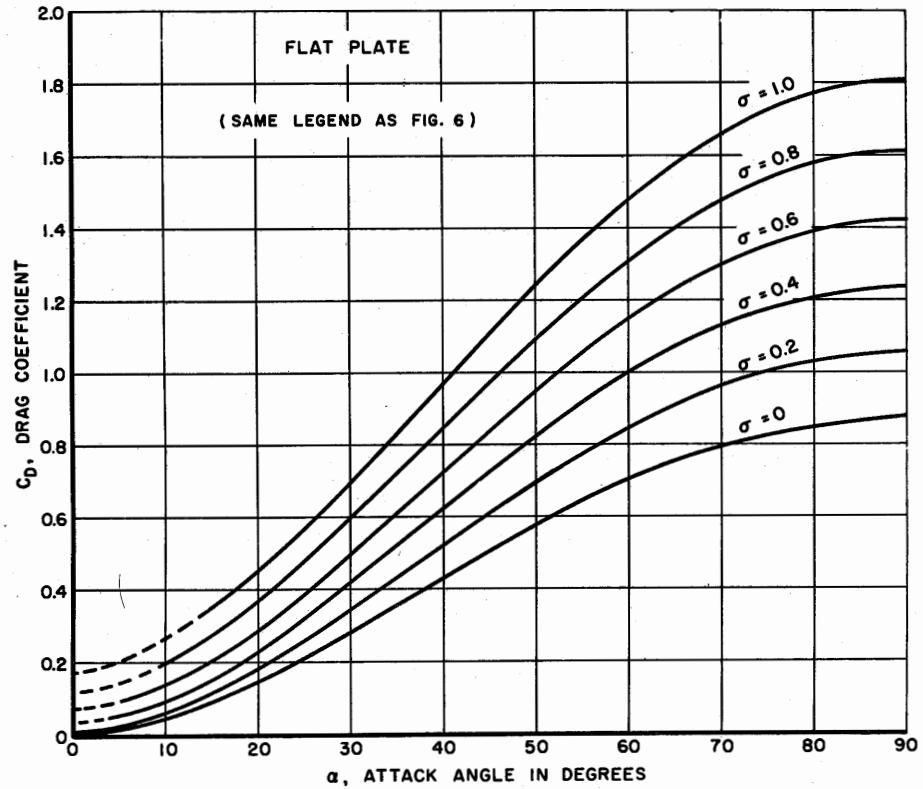

Fig. 7 - The dependence of C_D on α.

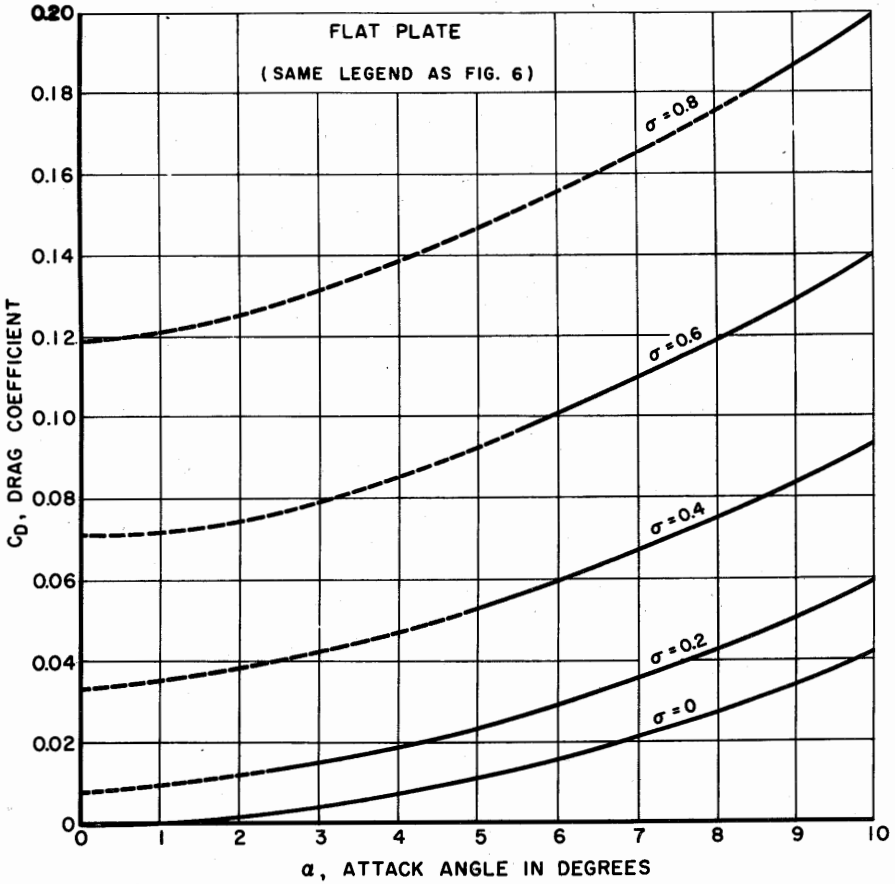

Fig. 8 - Values of C_D for small α.

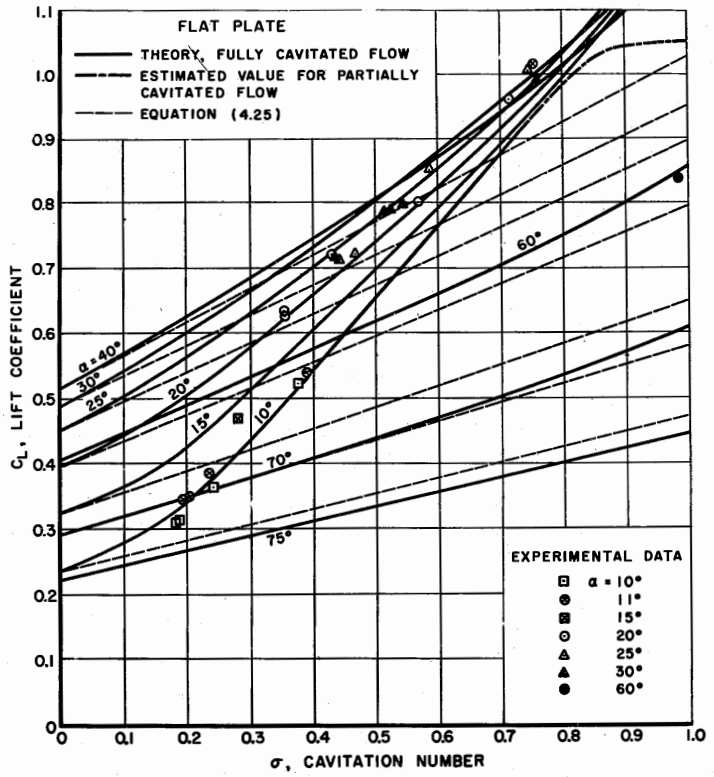

Fig. 9 - The dependence of C_L on σ.

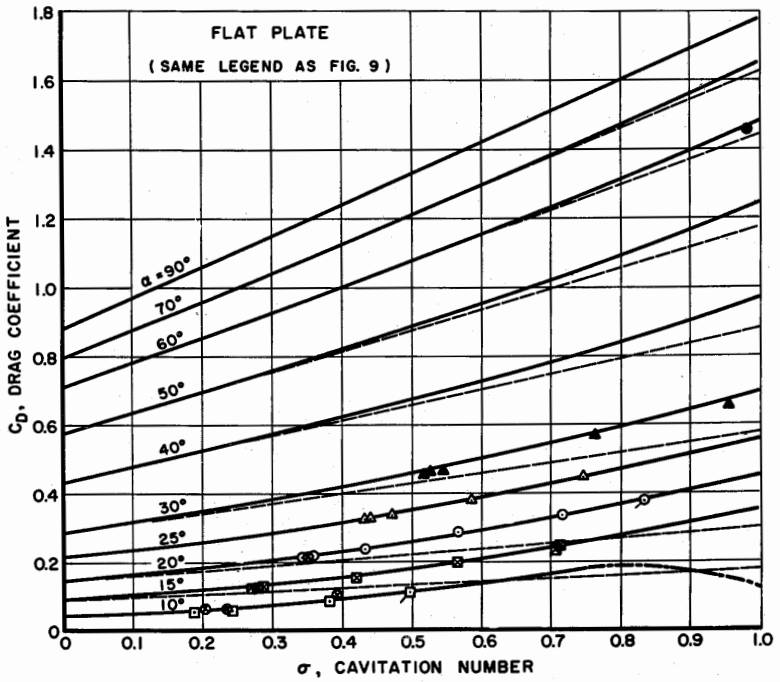

Fig. 10 - The dependence of C_D on σ.

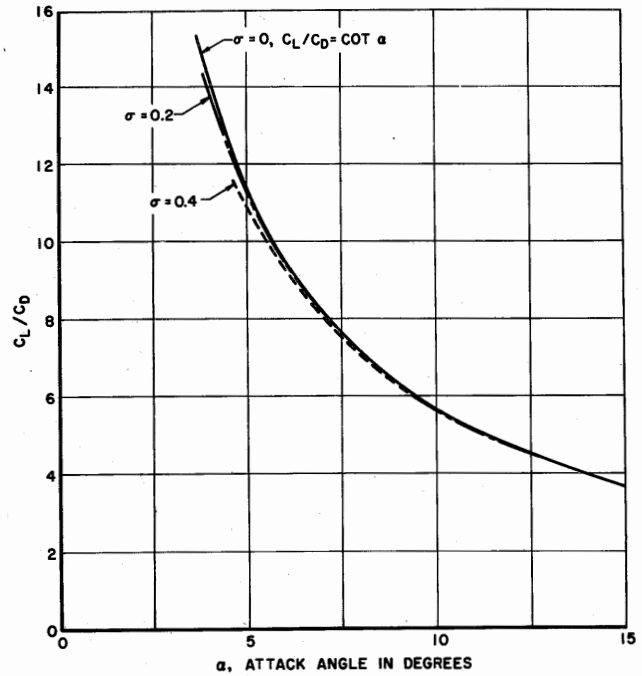

Fig. 11 - Values of C_L/C_D for the flat plate.

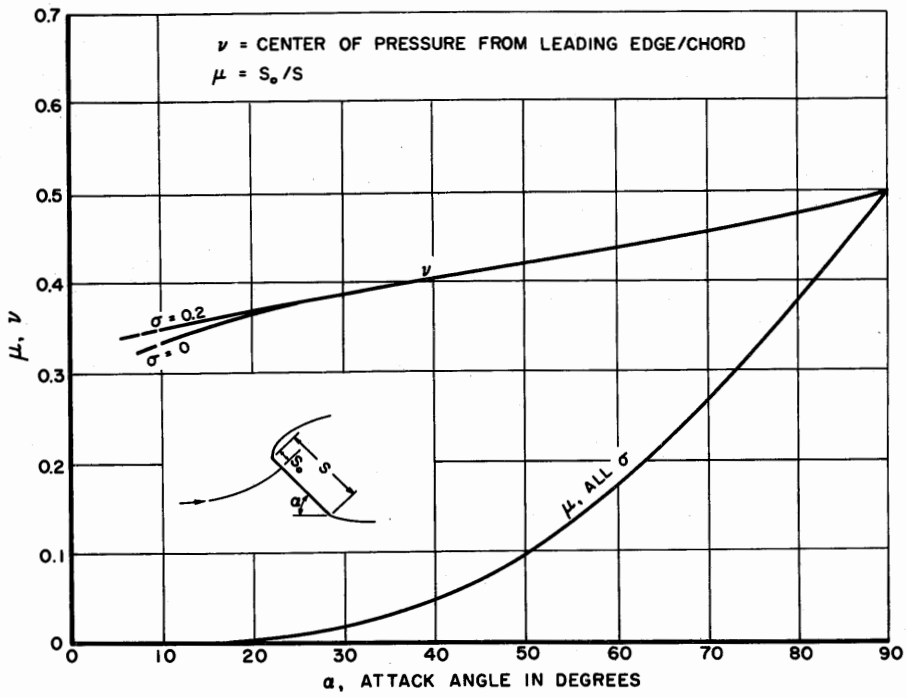

Fig. 12 - Location of stagnation point and center of pressure (flat plate).

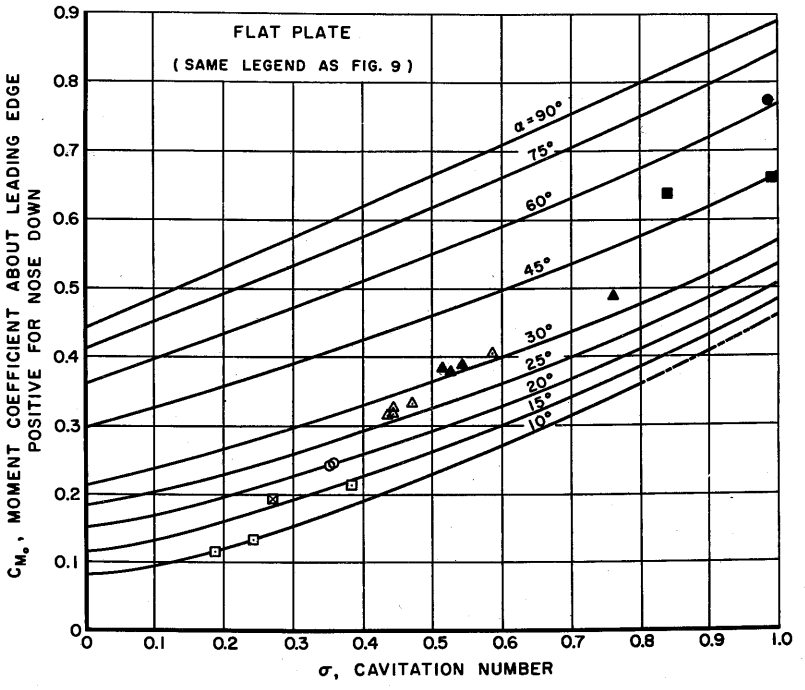

Fig. 13

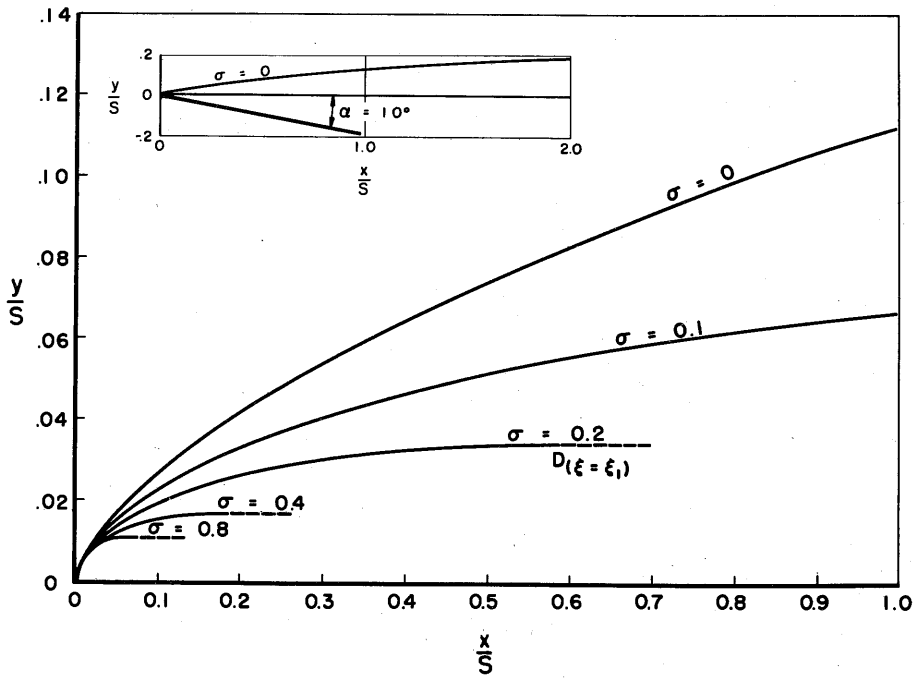

Fig. 14 - Some calculated locations of the free streamline.

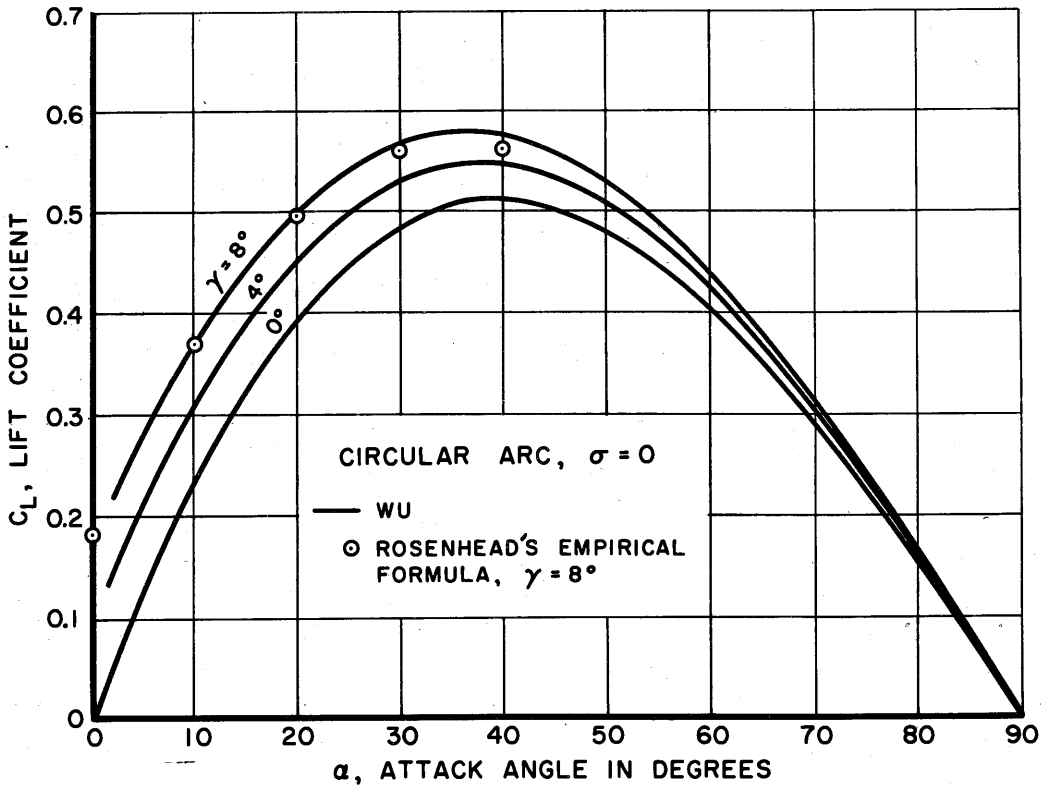

Fig. 15 - Effect of camber on C_L at $\sigma = 0$.

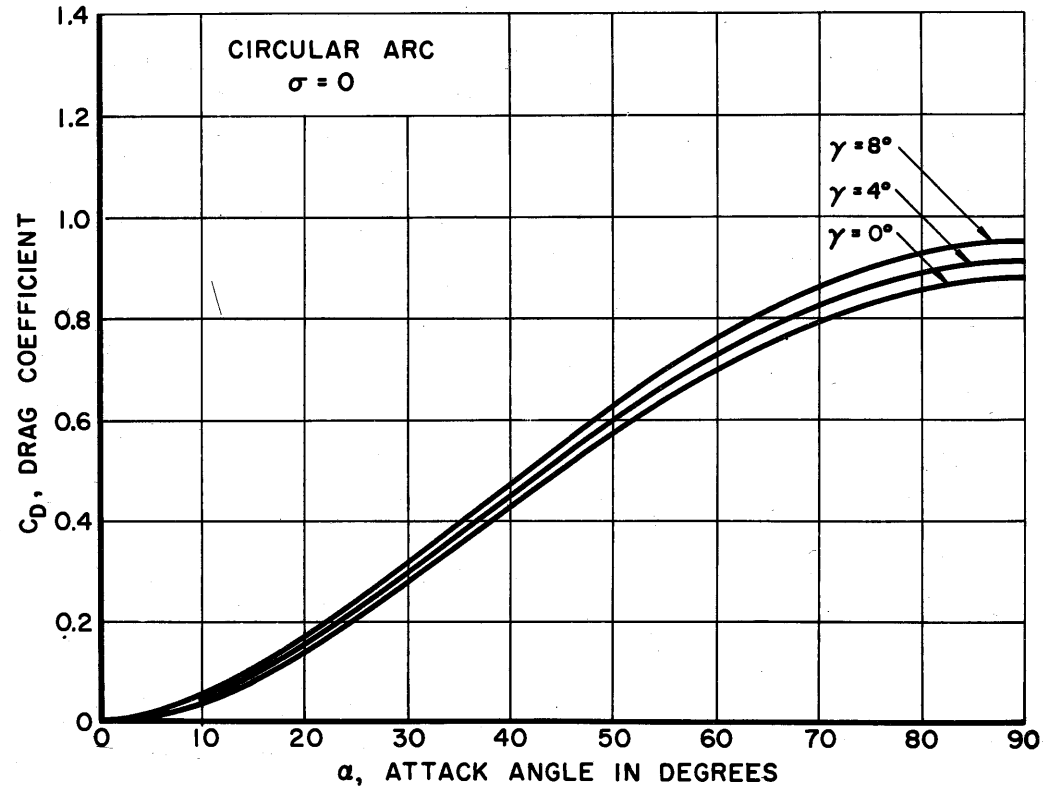

Fig. 16 - Effect of camber on C_D at $\sigma = 0$.

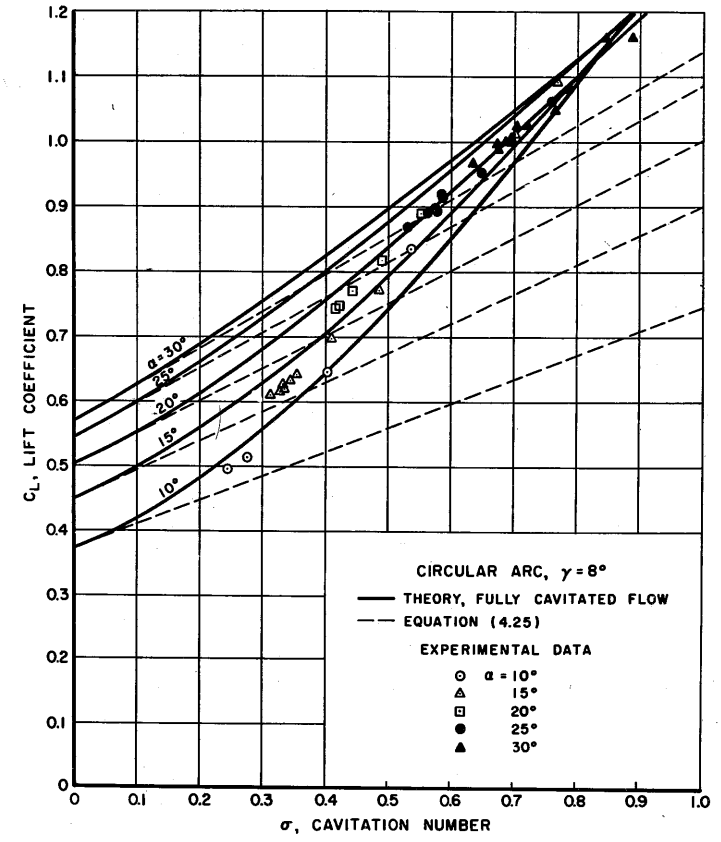
CIRCULAR ARC, γ = 8°
THEORY, FULLY CAVITATED FLOW
EQUATION (4.25)
EXPERIMENTAL DATA
α = 10°
15°
20°
25°
30°
α = 30°
25°
20°
15°
10°
C_L, LIFT COEFFICIENT
σ, CAVITATION NUMBER

Fig. 17

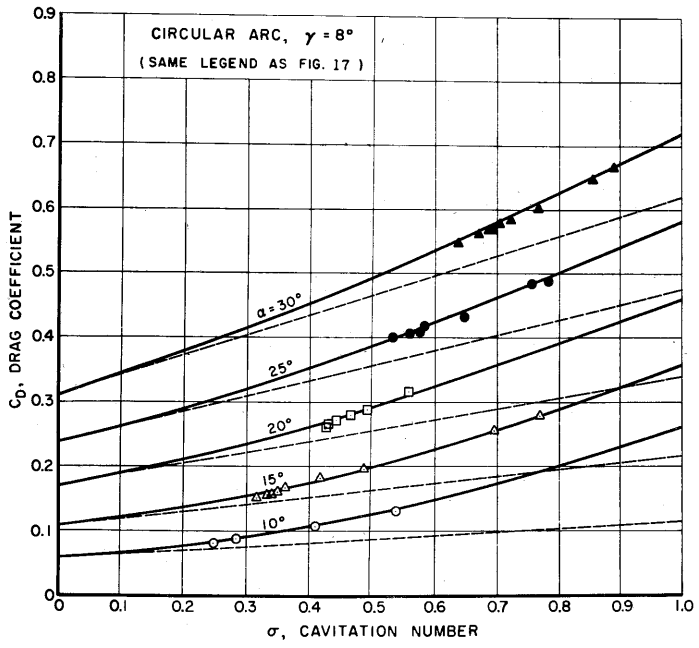
CIRCULAR ARC, γ = 8°
(SAME LEGEND AS FIG. 17)
α = 30°
25°
20°
15°
10°
C_D, DRAG COEFFICIENT
σ, CAVITATION NUMBER

Fig. 18

DISTRIBUTION LIST FOR UNCLASSIFIED
REPORTS ON CAVITATION
Contract N6onr-24420 (NR 062-059)

Chief of Naval Research
Navy Department
Washington 25, D.C.
Attn: Code 438 (3)
Code 463 (1)

Commanding Officer
Office of Naval Research
Branch Office
The John Crear Library Bldg.
86 E. Randolph Street
Chicago 1, Illinois (1)

Commanding Officer
Office of Naval Research
Branch Office
346 Broadway
New York 13, New York (1)

Commanding Officer
Office of Naval Research
Branch Office
1030 East Green Street
Pasadena 1, California (1)

Commanding Officer
Office of Naval Research
Navy 100, Fleet Post Office
New York, New York (5)

Director
Naval Research Laboratory
Washington 25, D.C.
Attn: Code 2021 (6)

Chief, Bureau of Aeronautics
Navy Department
Washington 25, D.C.
Attn: Research Division (1)
Aero and Hydro Branch
(Code Ad-3) (1)
Appl. Mech. Branch
(Code DE-3) (1)

Chief, Bureau of Ordnance
Navy Department
Washington 25, D.C.
Attn: Asst. Chief for Research
(Code Re) (1)
Systems Director, Underwater Ord (Code Rexc) (1)
Armor, Bomb, Projectile, Rocket, Guided Missile Warhead and Ballistics Branch
(Code Re3) (1)
Torpedo Branch (Code Re6) (1)
Research and Components Section (Code Re6a) (1)
Mine Branch (Code Re7) (1)

Chief, Bureau of Ships
Navy Department
Washington 25, D.C.
Attn: Research and Development (Code 300) (1)
Ship Design (Code 410) (1)
Preliminary Design and Ship Protection (Code 420) (1)
Scientific, Structural and Hydrodynamics (Code 442) (1)
Submarines (Code 525) (1)
Propellers and Shafting
(Code 554) (1)

Chief, Bureau of Yards and Docks, Navy Department
Washington 25, D.C.
Attn: Research Division (1)

Commander
Naval Ordnance Test Station
3202 E. Foothill Blvd.
Pasadena, California
Attn: Head, Underwater Ord. (1)
Head, Research Div. (1)

Commander
Naval Ordnance Test Station
Inyokern, China Lake, Calif.
Attn: Technical Library (1)

Commanding Officer and Director
David Taylor Model Basin
Washington 7, D.C.
Attn: Hydromechanics Lab. (1)
Seaworthiness and Fluid Dynamics Div. (1)
Library (1)

Commanding Officer
Naval Ordnance Laboratory
White Oak, Maryland
Attn: Underwater Ord. Dept. (1)

Commanding Officer
Naval Underwater Ordnance Sta.
Newport, Rhode Island (1)

Director
Underwater Sound Laboratory
Fort Trumbull
New London, Connecticut (1)

Librarian
U.S. Naval Postgraduate School
Monterey, California (1)

Executive Secretary
Research and Development Board
Department of Defense
The Pentagon
Washington 25, D.C. (1)

Chairman
Underseas Warfare Committee
National Research Council
2101 Constitution Avenue
Washington 25, D.C. (1)

Dr. J. H. McMillen
National Science Foundation
1520 H Street, N.W.
Washington, D.C. (1)

Director
National Bureau of Standards
Washington 25, D.C.
Attn: Fluid Mechanics Section (1)

Dr. G. H. Keulegan
National Hydraulic Laboratory
National Bureau of Standards
Washington 25, D.C. (1)

Director of Research
National Advisory Committee for Aeronautics
1512 H Street, N.W.
Washington 25, D.C. (1)

Director
Langley Aeronautical Laboratory
National Advisory Committee for Aeronautics
Langley Field, Virginia (1)

Mr. J. B. Parkinson
Langley Aeronautical Laboratory
National Advisory Committee for Aeronautics
Langley Field, Virginia (1)

Commander
Air Research and Development Command
P.O. Box 1395
Baltimore 18, Maryland
Attn: Fluid Mechanics Div. (1)

Director
Waterways Experiment Station
Box 631
Vicksburg, Mississippi (1)

Beach Erosion Board
U.S. Army Corps of Engineers
Washington 25, D.C. (1)

Office of Ordnance Research
Department of the Army
Washington 25, D.C. (1)

Office of the Chief of Engineers
Department of the Army
Gravelly Point
Washington 25, D.C. (1)

Commissioner
Bureau of Reclamation
Washington 25, D.C. (1)

Director
Oak Ridge National Laboratory
P.O. Box P
Oak Ridge, Tennessee (1)

Director
Applied Physics Division
Sandia Laboratory
Albuquerque, New Mexico (1)

Documents Service Center
Armed Services Technical
Information Agency
Knott Building
Dayton 2, Ohio (5)

Office of Technical Services
Department of Commerce
Washington 25, D.C. (1)

Polytechnic Institute of Brooklyn
Department of Aeronautical
Engineering and Applied Mech.
99 Livingston Street
Brooklyn 1, New York
Attn: Prof. H. Reissner (1)

Division of Applied Mathematics
Brown University
Providence 12, Rhode Island (1)

California Institute of Technology
Pasadena 4, California
Attn: Hydrodynamics Laboratory
Professor A. Hollander (1)
Professor R. T. Knapp (1)
Professor M. S. Plesset (1)
Professor V. A. Vanoni (1)
GALCIT
Prof. C.B. Millikan, Director (1)
Prof. Harold Wayland (1)

University of California
Berkeley 4, California
Attn: Professor H.A. Einstein
Dept. of Engineering (1)
Professor H. A. Schade,
Dir. of Engr. Research (1)

Case Institute of Technology
Department of Mechanical Engineering
Cleveland, Ohio
Attn: Professor G. Kuerti (1)

Cornell University
Graduate School of Aeronautical
Engineering
Ithaca, New York
Attn: Prof. W.R. Sears, Director(1)

Harvard University
Dept. of Mathematics
Cambridge 38, Mass.
Attn: Prof. G. Birkhoff (1)

University of Illinois
Dept. of Theoretical and
Applied Mechanics
College of Engineering
Urbana, Illinois
Attn: Dr. J. M. Robertson (1)

Indiana University
Dept. of Mathematics
Bloomington, Indiana
Attn: Professor D. Gilbarg (1)

State University of Iowa
Iowa Institute of Hydraulic
Research, Iowa City, Iowa
Attn: Dr. Hunter Rouse, Dir. (1)

University of Maryland
Inst. for Fluid Dynamics and
Applied Mathematics
College Park, Maryland
Attn: Prof. M. H. Martin,
Director (1)
Prof. J. R. Weske (1)

Massachusetts Institute of
Technology
Cambridge 39, Mass.
Attn: Prof. W.M. Rohsenow,
Dept. Mech. Engr. (1)
Prof. A.T. Ippen,
Hydrodynamics Laboratory (1)

Michigan State College
Hydraulics Laboratory
East Lansing, Michigan
Attn: Prof. H.R. Henry (1)

University of Michigan
Ann Arbor, Michigan
Attn: Director, Engineering
Research Institute (1)
Prof. V.L. Streeter,
Civil Engineering Dept. (1)

University of Minnesota
St. Anthony Falls Hydraulic Lab.
Minneapolis 14, Minnesota
Attn: Dr. L.G. Straub, Dir. (1)

New York University
Institute of Mathematical Sciences
25 Waverly Place
New York 3, New York
Attn: Prof. R. Courant, Dir. (1)

University of Notre Dame
College of Engineering
Notre Dame, Indiana
Attn: Dean K.E. Schoenherr (1)

Pennsylvania State University
Ordnance Research Laboratory
University Park, Pennsylvania
Attn: Prof. G.F. Wislicenus (1)

Rensselaer Polytechnic Inst.
Department of Mathematics
Troy, New York
Attn: Dr. Hirsh Cohen (1)

Stanford University
Stanford, California
Attn: Applied Mathematics and
Statistics Laboratory (1)
Prof. P.R. Garabedian (1)
Prof. L.I. Schiff, Dept. of
Physics (1)
Prof. J.K. Vennard, Dept.
of Civil Engineering (1)

Stevens Institute of Technology
Experimental Towing Tank
711 Hudson Street
Hoboken, New Jersey (1)

Worcester Polytechnic Institute
Alden Hydraulic Laboratory
Worcester, Massachusetts
Attn: Prof. J.L. Hooper,
Director (1)

Dr. Th. von Karman
1051 S. Marengo Street
Pasadena, California (1)

Aerojet General Corporation
6352 N. Irwindale Avenue
Azusa, California
Attn: Mr. C. A. Gongwer (1)

Dr. J.J. Stoker
New York University
Institute of Mathematical Sciences
25 Waverly Place
New York 3, New York (1)

Prof. C.C. Lin
Dept. of Mathematics
Massachusetts Institute of
Technology
Cambridge 39, Mass. (1)

Dr. Columbus Iselin
Woods Hole Oceanographic Inst.
Woods Hole, Mass. (1)

Dr. A.B. Kinzel, President
Union Carbide and Carbon Re-
search Laboratories, Inc.
30 E. 42nd St.
New York, N.Y. (1)

Dr. F.E. Fox
Catholic University
Washington 17, D.C. (1)

Dr. Immanuel Estermann
Office of Naval Research
Code 419
Navy Department
Washington 25, D.C. (1)

Goodyear Aircraft Corporation
Akron 15, Ohio
Attn: Security Officer (1)

Dr. F.V. Hunt
Director Acoustics Research
Laboratory
Harvard University
Cambridge, Mass. (1)

Prof. Robert Leonard
Dept. of Physics
University of California at L.A.
West Los Angeles, Calif. (1)

Prof. R.E.H. Rasmussen
Buddenvej 47, Lyngby
Copenhagen, Denmark
via: ONR, Pasadena, Calif. (1)